

We put science to work.™



**Savannah River
National Laboratory™**

OPERATED BY SAVANNAH RIVER NUCLEAR SOLUTIONS

A U.S. DEPARTMENT OF ENERGY NATIONAL LABORATORY • SAVANNAH RIVER SITE • AIKEN, SC

GoldSim® Aquifer Model Calibration and Plume Interaction

J. L. Wohlwend

G. P. Flach

March 28, 2018

SRNL-STI-2018-00160, Revision A

SRNL.DOE.GOV

DISCLAIMER

This work was prepared under an agreement with and funded by the U.S. Government. Neither the U.S. Government or its employees, nor any of its contractors, subcontractors or their employees, makes any express or implied:

1. warranty or assumes any legal liability for the accuracy, completeness, or for the use or results of such use of any information, product, or process disclosed; or
2. representation that such use or results of such use would not infringe privately owned rights; or
3. endorsement or recommendation of any specifically identified commercial product, process, or service.

Any views and opinions of authors expressed in this work do not necessarily state or reflect those of the United States Government, or its contractors, or subcontractors.

Printed in the United States of America

**Prepared for
U.S. Department of Energy**

Keywords: *GoldSim, E Area, Model, Aquifer, Plume Interaction, Calibration, Performance Assessment*

Retention: *Permanent*

GoldSim® Aquifer Model Calibration and Plume Interaction

J. L. Wohlwend
G. P. Flach

March 28, 2018

Prepared for the U.S. Department of Energy under contract number DE-AC09-08SR22470.



REVIEWS AND APPROVALS

AUTHORS:

J. L. Wohlwend, Environmental Modeling Date

G. P. Flach, Environmental Modeling Date

TECHNICAL REVIEW:

J. A. Dyer, Environmental Modeling, SRNL Date

APPROVAL:

D. A. Crowley, Manager Date
Environmental Modeling, SRNL

L. T. Reid, Acting Director, Environmental Restoration Technology, SRNL Date

ACKNOWLEDGEMENTS

This report documents the development and calibration of the GoldSim® Aquifer Model as well as implementation of plume interaction. The authors gratefully acknowledge J. A. Dyer, L. L. Hamm, and B. T. Butcher for their counsel.

EXECUTIVE SUMMARY

The E-Area Low-Level Waste Facility (ELLWF) Probabilistic Aquifer Model (PAM) utilizes GoldSim® Monte Carlo simulation software (GTG, 2017) to evaluate the transport of a tracer species as it travels from the water table below the disposal unit footprint, through the aquifer, to the Point of Assessment (POA) at the 100-meter boundary. This report documents the development and calibration of PAM as well as the implementation of plume interaction. PAM is a key component of the effort to include uncertainty quantification and sensitivity analysis (UQSA) in the next revision of the E-Area Performance Assessment (PA), considering recommendations from the 2015 PA strategic planning team outlined by Butcher and Phifer (2016). The Aquifer Model and associated optimized geometric parameters will be implemented in the future GoldSim® (GS) system model that will simulate subsurface flow and radionuclide transport from the ground surface to the 100-meter POA.

Simulations were performed to develop a methodology for calibrating PAM to PORFLOW (PF) tracer simulation results for both steady-state and pulse source terms. The East Aquifer Model had more disposal units (DUs) with errors over 5% and required additional calibration to better match PF results compared to the West and Center Aquifer Models. This is likely due to the plume traveling partially in the high-velocity transmissive zone (TZ) and the low-velocity tan clay confining zone (TCCZ) and lower aquifer zone (LAZ), as well as the streamtraces not being oriented perpendicular to the DU's cross-section. Overall percent errors, shown in Figure 0-1, between the calibrated Aquifer Model and the PF tracer simulations average 4% for the 32.8-foot and 10-foot dispersivity cases and 12% for the 100-foot dispersivity cases. Compared to the West and Center Aquifer Models, the East Aquifer Model has consistently larger Plume Overlap Factors with 22 factors exceeding 0.50 for the 32.8-foot dispersivity, steady-state simulations. As expected, the factors are larger where the streamtraces for neighboring DUs are nearby.

Key findings and recommendations include:

- Use of a single GS aquifer element for each DU adequately reproduces 3D PORFLOW tracer simulation results.
- Implementation of plume overlap will not utilize the built-in GS plume function because this correction factor requires calibration to the ratio between the PF-calculated plume contribution and the GS concentration. Instead, the ratio itself will be directly used as the Plume Overlap Factor (POF) as a simpler means of accounting for co-mingling of plumes.

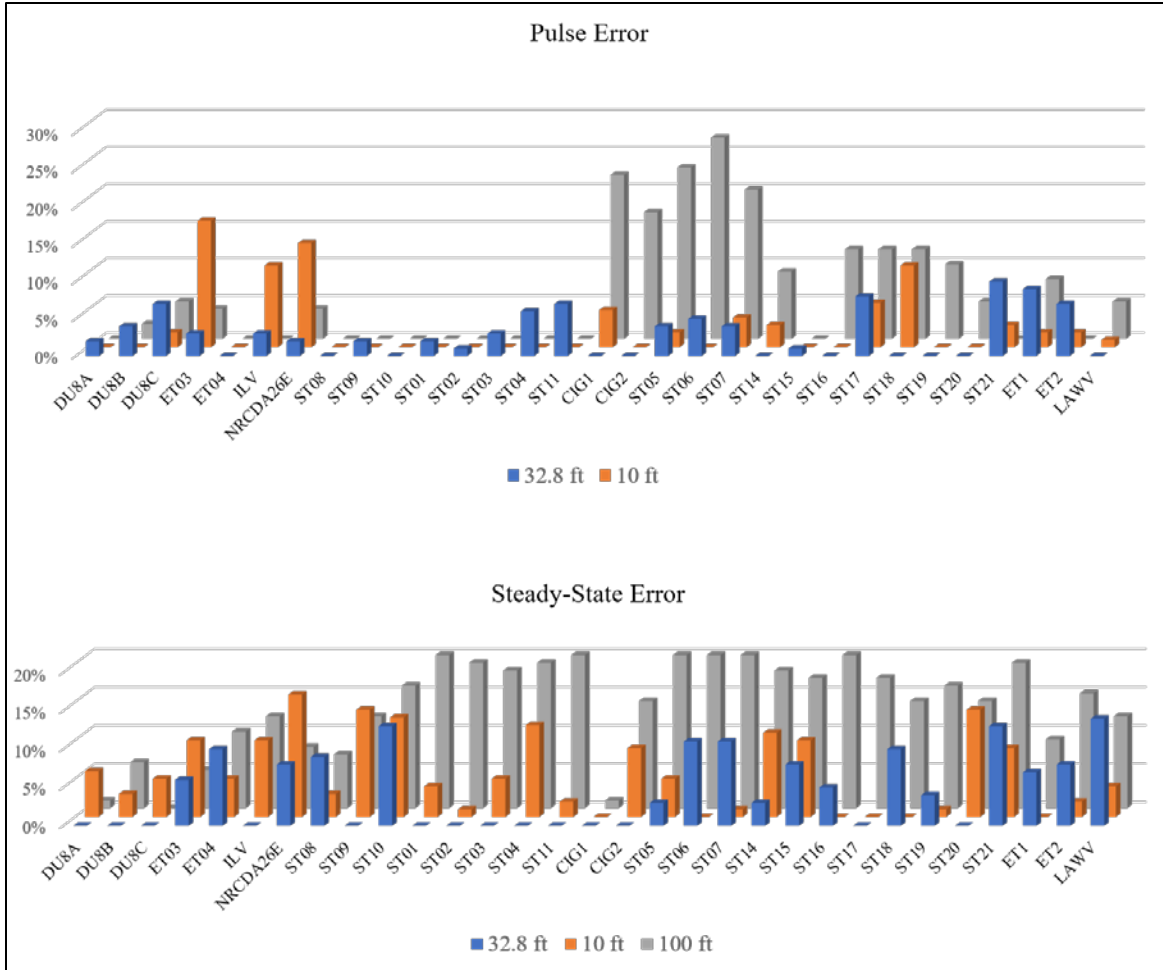


Figure 0-1. GS Aquifer Model pulse and steady-state source errors in tracer concentration compared to PF results

TABLE OF CONTENTS

LIST OF TABLES	ix
LIST OF FIGURES	ix
LIST OF ABBREVIATIONS.....	xi
1.0 Introduction.....	1
2.0 PORFLOW Reference Simulations	2
3.0 ELLWF Probabilistic Aquifer Model	5
3.1 Model Abstraction.....	5
3.2 Model Development.....	7
3.3 Calibration.....	12
3.4 Plume Interaction	15
4.0 Results.....	15
4.1 West Aquifer Model.....	15
4.1.1 Disposal Units 8A, 8B, & 8C	16
4.1.2 West Engineered Trenches	17
4.1.3 Intermediate Level Vault & Naval Reactor Component Disposal Area.....	18
4.1.4 West Slit Trenches.....	18
4.2 Center Aquifer Model	19
4.2.1 Center Slit Trenches	20
4.2.2 Components-in-Grout Trenches	20
4.3 East Aquifer Model	22
4.3.1 East Slit Trenches	22
4.3.2 East Engineered Trenches and Low-Activity Waste Vault	25
4.4 Plume Overlap Factors	26
4.4.1 West Aquifer Model	26
4.4.2 Center Aquifer Model.....	28
4.4.3 East Aquifer Model.....	29
5.0 Conclusions.....	30
6.0 References.....	32
Appendix A . GS Aquifer Model Pulse Source Plume Overlap Functions	A-1

LIST OF TABLES

Table 2-1. Travel distance, travel time, and Darcy velocity from streamtraces	5
Table 4-1. West Aquifer Model concentration and time-of-peak errors	16
Table 4-2. Calibrated West Aquifer Model geometric parameter multiplier values.....	16
Table 4-3. Center Aquifer Model concentration and time-of-peak errors	19
Table 4-4. Calibrated Center Aquifer Model geometric parameter multiplier values	20
Table 4-5. East Aquifer Model concentration and time-of-peak errors	23
Table 4-6. Calibrated East Aquifer Model geometric parameter multiplier values	23
Table 4-7. West Aquifer Model’s plume overlap factors: 32.8-foot dispersivity, steady-state source.....	27
Table 4-8. West Aquifer Model’s plume overlap factors: 10-foot dispersivity, steady-state source.....	27
Table 4-9. West Aquifer Model’s plume overlap factors: 100-foot dispersivity, steady-state source.....	27
Table 4-10. Center Aquifer Model’s plume overlap factors: 32.8-foot dispersivity, steady-state source ..	28
Table 4-11. Center Aquifer Model’s plume overlap factors: 10-foot dispersivity, steady-state source	28
Table 4-12. Center Aquifer Model’s plume overlap factors: 100-foot dispersivity, steady-state source ..	28
Table 4-13. East Aquifer Model’s plume overlap factors: 32.8-foot dispersivity, steady-state source	29
Table 4-14. East Aquifer Model’s plume overlap factors: 10-foot dispersivity, steady-state source	30
Table 4-15. East Aquifer Model’s plume overlap factors: 100-foot dispersivity, steady-state source	30

LIST OF FIGURES

Figure 0-1. GS Aquifer Model pulse and steady-state source errors in tracer concentration compared to PF results.....	vii
Figure 1-1. E-Area LLW Facility disposal units (unlabeled numbered units are slit trenches; ET units are engineered trenches; CIG units are component-in-grout trenches; ILV is the intermediate level vault; LAWV is the low-activity waste vault; 7E and 26E are naval reactor component disposal areas; 8A, 8B, and 8C are future slit or engineered trenches)	2
Figure 2-1. West, Center, and East refinements of the GSA2016 grid.....	4
Figure 3-1. Illustration of the aquifer submodels in PAM. The blue overlapping squares represent the PORFLOW boundaries, the red polygons represent the disposal units and the grey-shaded areas represent the disposal units not implemented in the submodel.....	7
Figure 3-2. Screen shot of the West Aquifer Model; each disposal unit is enclosed in a localized container	8

Figure 3-3. GoldSim® Aquifer Model template 9

Figure 3-4. GoldSim® aquifer element illustrating some of the required geometric variables 10

Figure 3-5. Tecplot representation of the steady-state PORFLOW results utilized in estimating the source length and aquifer area *(Note the different views do not have the same magnification) 11

Figure 3-6. Schematic representation of the aquifer element 11

Figure 3-7. Parameter subfolder showing the variables utilized in the calibration procedure..... 12

Figure 3-8. Optimization screens showing input parameters..... 13

Figure 3-9. Calibration flow diagram 13

Figure 3-10. Example results from a successful “simple” calibration (dashed = PF, solid = GS)..... 14

Figure 3-11. GS results showing concentration profiles before and after manual calibration..... 14

Figure 3-12. Schematic of plume interaction..... 15

Figure 4-1. GS POA concentrations for DU 8A-C compared to PF results..... 17

Figure 4-2. GS POA concentrations for ET 3 and 4 compared to PF results..... 17

Figure 4-3. GS POA concentrations for ILV and NRCDA 26E compared to PF results 18

Figure 4-4. GS POA concentrations for ST 8-10 compared to PF results 19

Figure 4-5. GS POA concentrations for ST 1-4 & 11 compared to PF results 21

Figure 4-6. GS POA concentrations for CIG 1 & 2 compared to PF results 22

Figure 4-7. GS POA concentrations for ST 5, 6, 7, 14 and 16 compared to PF results..... 24

Figure 4-8. GS POA concentrations for ST 17, 18, 19, 20, and 21 compared to PF results..... 25

Figure 4-9. GS POA concentrations for ET 1 & 2 and LAWV compared to PF results..... 26

Figure 5-1. GS Aquifer Model pulse and steady-state source errors in tracer concentration compared to PF results..... 31

LIST OF ABBREVIATIONS

CA	Composite Analysis
CIG	Components-in-Grout
DOE	Department of Energy
DU	Disposal Unit
ELLWF	E-Area Low-Level Waste Facility
ET	Engineered Trench
ft	feet
GS	GoldSim®
GSA	General Separations Area
ILV	Intermediate Level Vault
LAWV	Low Activity Waste Vault
LAZ	Lower Aquifer Zone
LFRG	Department of Energy's Low-Level Waste Disposal Facility Federal Review Group
LLW	Low-Level Waste
m	meter
NRCDA	Naval Reactor Component Disposal Area
PA	Performance Assessment
PAM	Probabilistic Aquifer Model
PF	PORFLOW
PO	Performance Objective
POA	Point of Assessment
POF	Plume Overlap Factor
SRNL	Savannah River National Laboratory
SRS	Savannah River Site
SS	steady-state
ST	Slit Trench
TCCZ	Tan Clay Confining Zone
TOP	Time-of-Peak
TZ	Transmissive Zone
UQSA	Uncertainty Quantification and Sensitivity Analysis
yr	year

1.0 Introduction

The E-Area Low-Level Waste Facility (ELLWF) Probabilistic Aquifer Model (PAM) utilizes GoldSim[®] Monte Carlo simulation software (GTG, 2017) to evaluate the transport of a tracer radionuclide as it travels from the water table below the disposal unit footprint, through the aquifer, to the Point of Assessment (POA) at the 100-meter boundary. DOE Manual 435.1-1 stipulates “The performance assessment shall include a sensitivity/uncertainty analysis.” This model is part of the effort to address recommendations from the 2015 PA strategic planning team outlined by Butcher and Phifer (2016) to include uncertainty quantification and sensitivity analysis (UQSA) in the next revision of the ELLWF Performance Assessment (PA). UQSA is necessary to provide a reasonable expectation that the Performance Objectives (PO) will be met. PAM was developed as an initial step in implementing UQSA and contains the aquifer region beneath all E-Area disposal units (Figure 1-1). This report details the development of the model as well as the calibration procedure, including benchmarking comparisons of the breakthrough curves predicted by PORFLOW (PF) and GoldSim[®] (GS).

The 2009 Composite Analysis (CA) model parameterization (Hamm, 2009) utilized from the General Separations Area (GSA) flow model approximately 1,000 three-dimensional (3D) PF streamtraces emanating from each disposal unit to the POA. From these simulations, average one-dimensional (1D) aquifer parameters were obtained for each unit in addition to statistical information. PAM, on the other hand, obtains the GS aquifer parameters from PF tracer simulations. Specifically, GS parameters are calibrated to tracer breakthrough curves at the nodes having the maximum concentrations at the POA.

This report discusses benchmarking between the deterministic PF model and the stochastic GS model run in deterministic mode. PF is a higher-fidelity simulation of multi-dimensional transport phenomena while GS is a 1D transport model with a much lower computational time. Therefore, calibration to PF results is necessary to obtain accurate abstractions and to quantify the GS model systemic bias resulting from reduced dimensionality. The initial work to address the Department of Energy (DOE) Low-Level Waste (LLW) Disposal Facility Federal Review Group’s (LFRG) recommendations is to (1) create a new aquifer model using the GS simulation software (GTG, 2017), (2) develop the method for calibration, and (3) understand the sensitivity of the 100-meter POA concentration to the geometric variables utilized in the model. PAM simulates the subsurface advective transport of a tracer through the aquifer from the water table beneath each disposal unit (DU) to the POA at the 100-meter boundary.

PAM addresses only the aquifer portion of solute transport and can model several disposal units (DUs) in a single simulation. When modeling several DUs, the contribution of neighboring units (i.e., plume interactions) can be considered. To evaluate ELLWF plume interactions, a correction ratio based directly on PF and GS POA breakthrough results is used, instead of implementing the built-in “plume function” feature in GS. The rationale for this approach was to minimize the additional effort required to calibrate the plume function variables. This report, therefore, focuses on the calibration of geometric parameters utilized in the GS Aquifer Model using plume centerline concentrations.



Figure 1-1. E-Area LLW Facility disposal units (unlabeled numbered units are slit trenches; ET units are engineered trenches; CIG units are component-in-grout trenches; ILV is the intermediate level vault; LAWV is the low-activity waste vault; 7E and 26E are naval reactor component disposal areas; 8A, 8B, and 8C are future slit or engineered trenches)

2.0 PORFLOW Reference Simulations

The most recent groundwater flow model of the General Separations Area (GSA) was developed in 2016 – 2017 by Flach et al. (2017) and is referred to as the “GSA2016” model. The GSA2016 model reflects updated characterization and monitoring data, and use of the PEST optimization code to perform model calibration. The DOE LFRG recommended automated calibration in a 2008 review of the ELLWF PA (Bagwell and Flach, 2016). The final calibration phase produced four variants termed “GSA2016.LU,” “GSA2016.LW,” “GSA2016.HU,” and “GSA2016.HW,” where

- “L” = Layer-cake conductivity field
- “H” = Heterogeneous conductivity field
- “U” = Unweighted calibration targets
- “W” = Weighted calibration targets

The GSA2016.LW flow field was identified as the best-estimate calibration result and recommended for baseline analysis. The remaining three flow fields were recommended for uncertainty quantification and

sensitivity analysis. Thus, the GSA2016.LW model was chosen as the reference for GS Aquifer Model development.

Flach (2018a) recommended refinement of the GSA2016 grid and velocity field to a horizontal grid resolution of 25 feet (ft) and a vertical resolution of approximately 3 ft, to avoid significant numerical dispersion in solute transport simulations supporting the next revision of the ELLWF PA. Refining the entire GSA2016 grid to this resolution would create far too many grid cells for available computing resources, and be unnecessary for transport confined to E-Area. Therefore, refinement is typically confined to a reduced model extent. Feasible mesh sizes can be achieved by dividing E-Area into the overlapping “West,” “Center” and “East” footprints shown in Figure 2-1. Mesh and velocity field refinement is currently performed using the MESH3D code (Danielson, 2017). Also shown in Figure 2-1 are simulated groundwater pathlines and the 100-meter perimeter. The three overlapping cutouts are collectively capable of simulating solute transport from any E-Area DU to the 100-meter compliance boundary.

As discussed by Flach (2018a), groundwater modeling practitioners generally assume a longitudinal dispersivity, α_L , that is 10% (10^{-1}) of the plume travel distance L , unless site-specific data or conditions indicate otherwise. Plume travel distances in E-Area range from 100 meters (m) to several hundred meters, and are typically around 200 m. A representative range, excluding East DUs, is $100 \text{ m} \leq \alpha_L \leq 200 \text{ m}$, or $328 \text{ ft} \leq \alpha_L \leq 656 \text{ ft}$. The corresponding dispersivity range under the 10% rule-of-thumb is $32.8 \text{ ft} \leq \alpha_L \leq 65.6 \text{ ft}$. Considering data uncertainty, Flach (2018a) notes that a lower α_L equal to $3.16\%L$ ($10^{-1.5}L$) is also a credible setting. For $100 \text{ m} \leq L \leq 200 \text{ m}$, the lower dispersivity range is $3.16 \text{ m} \leq \alpha_L \leq 6.32 \text{ m}$, or approximately $10 \text{ ft} \leq \alpha_L \leq 20 \text{ ft}$. Considering variability in both α_L/L and L , three dispersivity values are considered representative of variability in α_L :

- $\alpha_L = 10 \text{ ft}$ approximately one-half order of magnitude lower than 32.8 ft
- $\alpha_L = 32.8 \text{ ft}$ minimum L and $\alpha_L/L = 10\%$
- $\alpha_L = 100 \text{ ft}$ approximately one-half order of magnitude larger than 32.8 ft

To provide reference results for GS Aquifer Model development, transport simulations were performed for each E-Area DU with $\alpha_L = 10 \text{ ft}$, 32.8 ft , and 100 ft . Because sorption affects the timing but not the shape of a solute plume (see Flach, 2018b), plume simulations were conducted with a non-sorbing tracer species. Two simulations were performed for each DU. The “Steady-State” (SS) simulation assumed a constant tracer source of 1.0 gram per year (g/yr) in source cells within the DU footprint and residing just beneath the water table. The simulation was run until steady-state conditions were achieved. The “Pulse” simulation assumed instantaneous placement of 1 gram (g) tracer in aquifer source cells, leading to a pulse of solute traveling toward the 100-meter perimeter. Tracer breakthrough was monitored at the 100-meter boundary. The time step was set to 0.1 years in the simulations to avoid significant numerical dispersion. PF results are compared to GoldSim® predictions in the next section. To guide initial parameterization of PAM, streamtraces emanating from the centers of DUs were analyzed for travel distance and time to the 100-meter POA. Table 2-1 summarizes travel distance, s , travel time, t , and calculated average Darcy velocity, U .

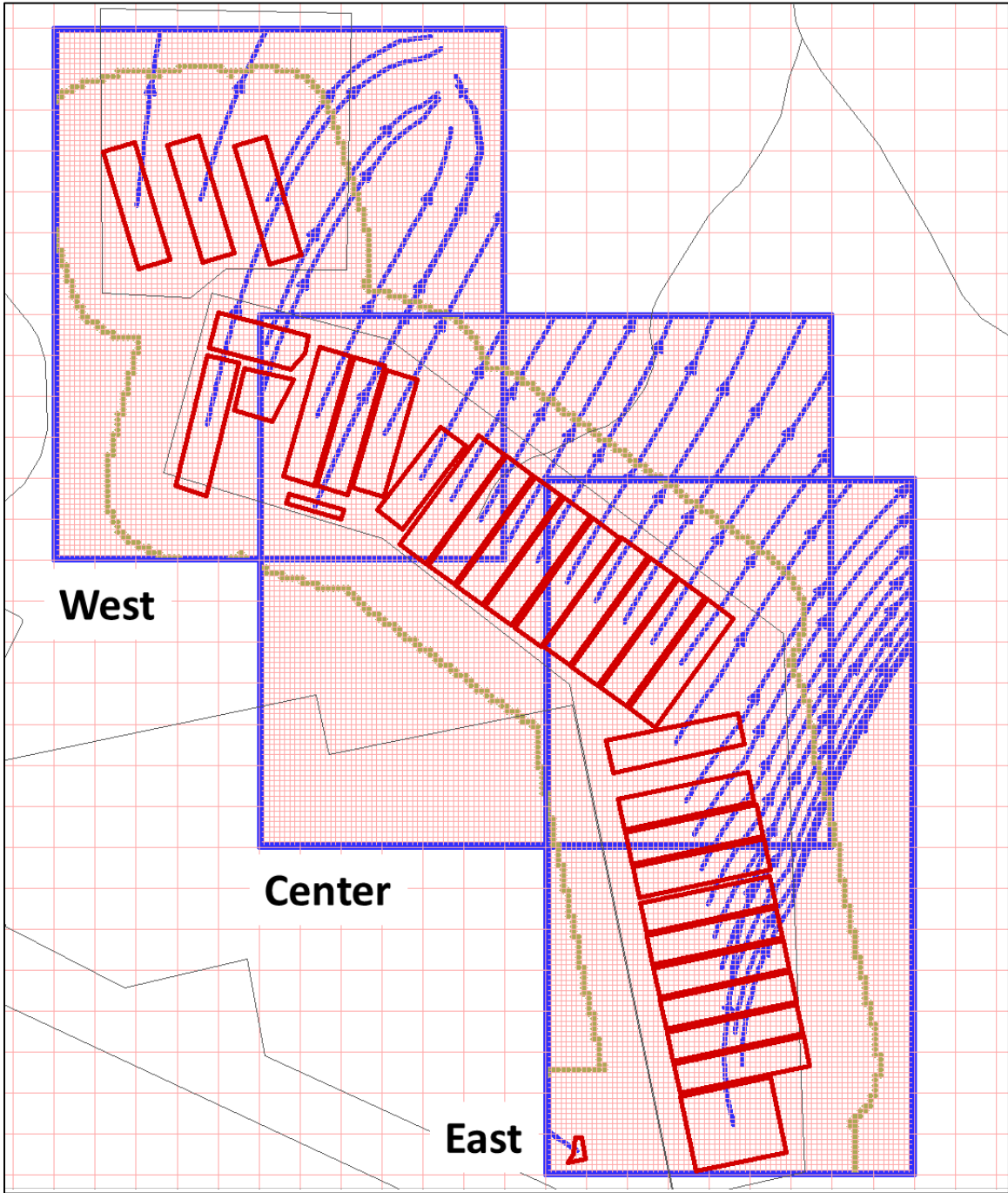


Figure 2-1. West, Center, and East refinements of the GSA2016 grid

Table 2-1. Travel distance, travel time, and Darcy velocity from streamtraces

TransportEast				TransportCenter				TransportWest			
DU	s (m)	t (yr)	U ¹ (m/yr)	DU	s (m)	t (yr)	U ¹ (m/yr)	DU	s (m)	t (yr)	U ¹ (m/yr)
				ST01	209	7.20	7.26				
				ST02	208	8.28	6.28				
				ST03	208	9.00	5.77				
				ST04	211	9.36	5.63				
ST05	208	9.14	5.69	ST05	207	9.11	5.67				
ST06	208	10.18	5.12	ST06	208	10.18	5.12				
ST07	207	10.47	4.94	ST07	208	10.50	4.96				
								ST08	206	5.11	10.07
								ST09	207	5.01	10.36
				ST10	196	4.86	10.07	ST10	198	4.92	10.09
				ST11	196	5.79	8.46	ST11	200	5.87	8.5
ST14	290	15.70	4.62	ST14	290	15.70	4.62				
ST15	307	15.53	4.94								
ST16	334	17.38	4.81								
ST17	342	17.86	4.79								
ST18	361	18.88	4.78								
ST19	387	19.71	4.9								
ST20	424	21.91	4.83								
ST21	600	29.59	5.07								
				CIG1	209	9.09	5.75				
CIG2	209	9.31	5.61	CIG2	208	9.28	5.59				
ET01	331	14.34	5.77	ET01	331	14.34	5.77				
ET02	307	12.31	6.23	ET02	305	12.28	6.21				
								ET03	282	6.52	10.8
								ET04	500	12.98	9.63
LAWV	325	16.36	4.97								
								ILV	338	9.96	8.49
								NRCD			
								A26E	335	8.22	10.19
								DU8A	200	5.05	9.89
								DU8B	207	4.74	10.91
								DU8C	173	3.41	12.68

¹ U (m/yr) = (η_{eff})(s)/t where η_{eff} (effective porosity) = 0.25.

3.0 ELLWF Probabilistic Aquifer Model

3.1 Model Abstraction

PORFLOW and GoldSim® solve the same solute transport equation representing advection, diffusion, dispersion, linear sorption, and radioactive (first-order) decay and ingrowth processes. Therefore, no abstraction of PF physical processes is required in developing a GS model. However, PF simulates three-dimensional transport using a 3D flow field, while GS simulates 1D transport in a constant-area streamtube using an average (Darcy) flow velocity. Reducing dimensionality from 3D to 1D introduces geometric abstraction challenges, even in the simplest case.

Suppose the velocity field is spatially uniform (constant) and the solute originates from injection of a fixed tracer mass at a point. The peak concentration, C_{peak}^{3D} , of the moving solute pulse in three dimensions is (Crank, 1975, Equation 3.5):

$$C_{peak}^{3D}(t) = \frac{M/n}{(4\pi^3\sqrt{D_L D_T D_V t})^{3/2}} = \frac{M/n}{(4\pi^3\sqrt{\alpha_L \alpha_T \alpha_V vt})^{3/2}} \quad (1)$$

where M is the mass of the solute; n is the porosity; D_L , D_T , and D_V are the diffusion coefficients in the longitudinal, transverse, and vertical directions, respectively; α_L , α_T , and α_V are the dispersivities in the longitudinal, transverse, and vertical directions, respectively; v is the velocity; and t is time.

Typical assumptions for the transverse dispersivities are (see Flach, 2018a):

$$\alpha_T = 0.1\alpha_L \quad (2)$$

$$\alpha_V = 0.01\alpha_L \quad (3)$$

Combining Equations (1) through (3) yields:

$$C_{peak}^{3D}(t) = \frac{M/n}{(4\pi 0.1\alpha_L vt)^{3/2}} \propto (\alpha_L vt)^{-1.5} \quad (4)$$

For one dimension, the peak concentration of the moving solute pulse is given by Bear (1972, Equation 10.6.10) and Crank (1975, Equation 2.6):

$$C_{peak}^{1D}(t) = \frac{M/n}{(4\pi D_L t)^{1/2}} = \frac{M/n}{(4\pi\alpha_L vt)^{1/2}} \propto (\alpha_L vt)^{-0.5} \quad (5)$$

The exponents in Equations (4) and (5) differ by a factor of 3 because dispersion is occurring in three directions versus one direction, respectively. The differing proportionalities have an important implication for GS model calibration. For a specific longitudinal dispersivity value (and velocity and distance/time), GS flow area can be adjusted to achieve agreement with GSA2016 or another 3D model. However, this calibration will not be valid at other dispersivity settings because Equations (4) and (5) have a different functional dependence on α_L . Rather, each dispersivity requires a separate calibration.

The flow field in the above scenario ($v = \text{constant}$) is easily abstracted to a 1D streamtube. Additional abstraction challenges occur when the flow field is more complicated. The water table resides above the tan clay confining zone (TCCZ) in roughly the eastern half of E-Area. Both hydraulic conductivity and pore velocity are significantly higher in the transmissive zone (TZ) above the TCCZ. Between a DU in this region and the 100-meter POA, part of the plume travels horizontally in the TZ while the remainder crosses the TCCZ and descends into the lower aquifer zone (LAZ). As discussed later in the report, this multi-dimensional behavior can be difficult to reproduce in a 1D streamtube.

3.2 Model Development

Similar to the PF overlapping, West, Center, and East footprints, PAM comprises three submodels containing several DUs each as shown in Figure 3-1. The illustration shows each DU represented by red polygons and the PF simulation boundaries outlined in blue. The grey shaded regions indicate DUs that were not included in the indicated submodel because they were implemented in a neighboring submodel. An example of the arrangement of individual DUs as localized containers is given in Figure 3-2. Each DU is created inside a localized container to simplify development because many parameters use the same name within each DU. If the container was not localized, unit-specific nomenclature would be required. Each model realization produces results for all DUs and allows for the evaluation of plume overlap. Two different aquifer pathways are created for each dispersion value, representing a steady-state and pulse source. Consistent with the PF reference simulations, the steady-state source assumes a 1 gram per year constant mass rate while the pulse source assumes a 1 gram initial inventory. Each pathway is represented by three elements: an inlet cell, an aquifer element composed of multiple internal cells, and a sink cell. The aquifer element has several input values that are utilized for calibration.

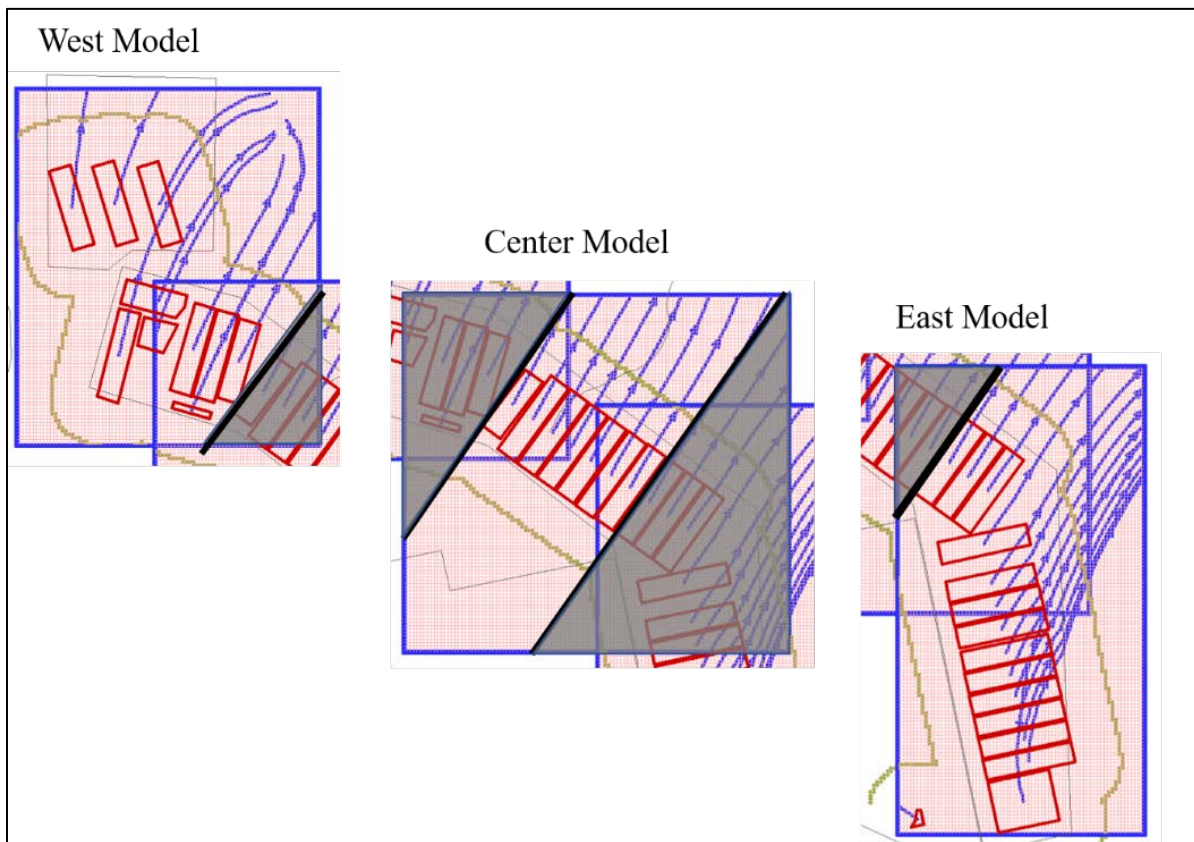


Figure 3-1. Illustration of the aquifer submodels in PAM. The blue overlapping squares represent the PORFLOW boundaries, the red polygons represent the disposal units and the grey-shaded areas represent the disposal units not implemented in the submodel

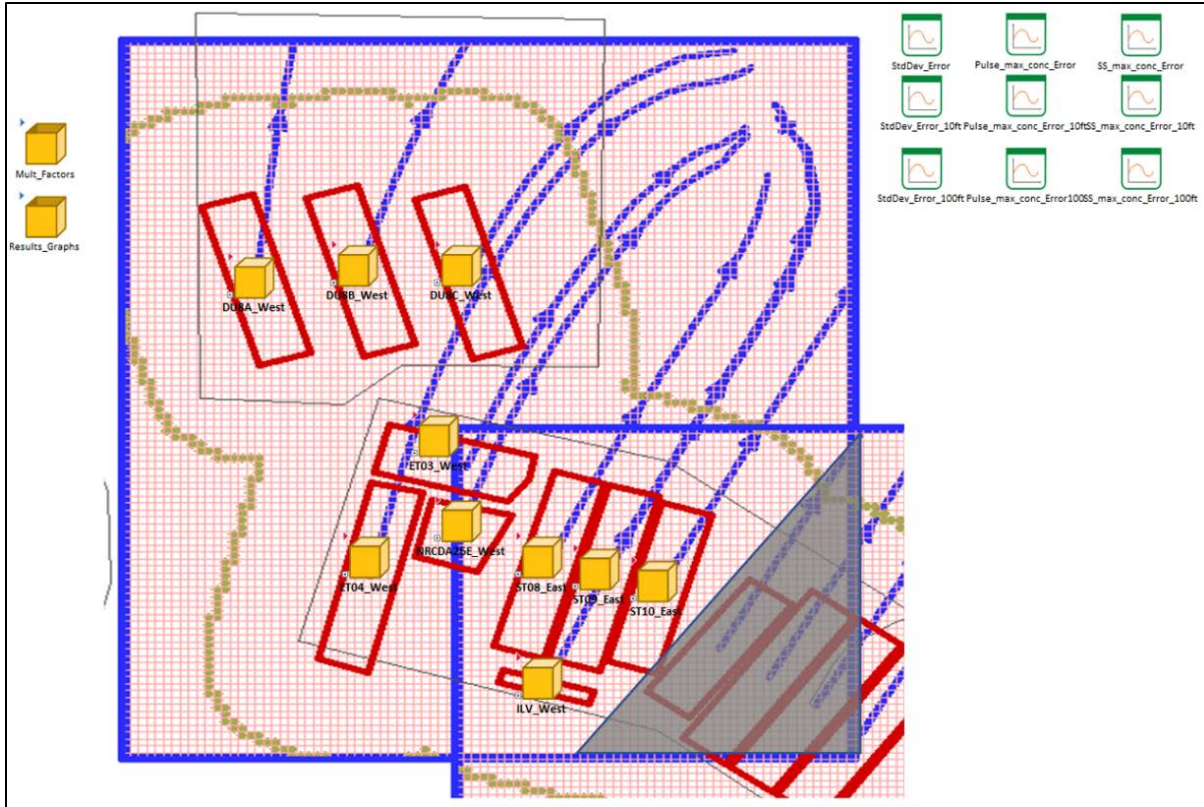


Figure 3-2. Screen shot of the West Aquifer Model; each disposal unit is enclosed in a localized container

Each DU utilizes the same template (Figure 3-3), only varying the geometric parameters and PF tracer results. The conceptual model implemented within the aquifer element is a row of linked computational cells having no-flow boundaries on the top, bottom and sides, allowing 1D transport solely in the aquifer flow direction. In the 2009 CA model (SRNL, 2009), the aquifer was composed of 200 cells, of which 100 represented the area directly beneath the waste zone footprint, 40 were mixed sandy/clayey soil cells, and 60 were sandy soil cells. In the current model, only a single aquifer element is used. While this cuts down the computational cost, it also constrains the aquifer to have a single infill medium. This restriction does not influence E-Area simulations because no streamtube encounters the Gordon confining unit clay zone. During the simulation, the aquifer element creates a temporary set of linked cell elements that represent the aquifer pathway.

Each aquifer element contains several geometric and transport parameters (the aquifer element data entry screen is shown in Figure 3-4) to simulate the entire aquifer zone, including a source region where the tracer species is uniformly placed. Figure 3-5 is a Tecplot representation of steady-state PF results utilized to estimate the source-zone length and aquifer area. The overall aquifer element length is the summation of the PF streamtrace travel distance, s (Table 2-1) and one-half the source zone length estimate ($SourceZone_{length}$), because the streamtrace simulations place the tracer source at the center of the DU.

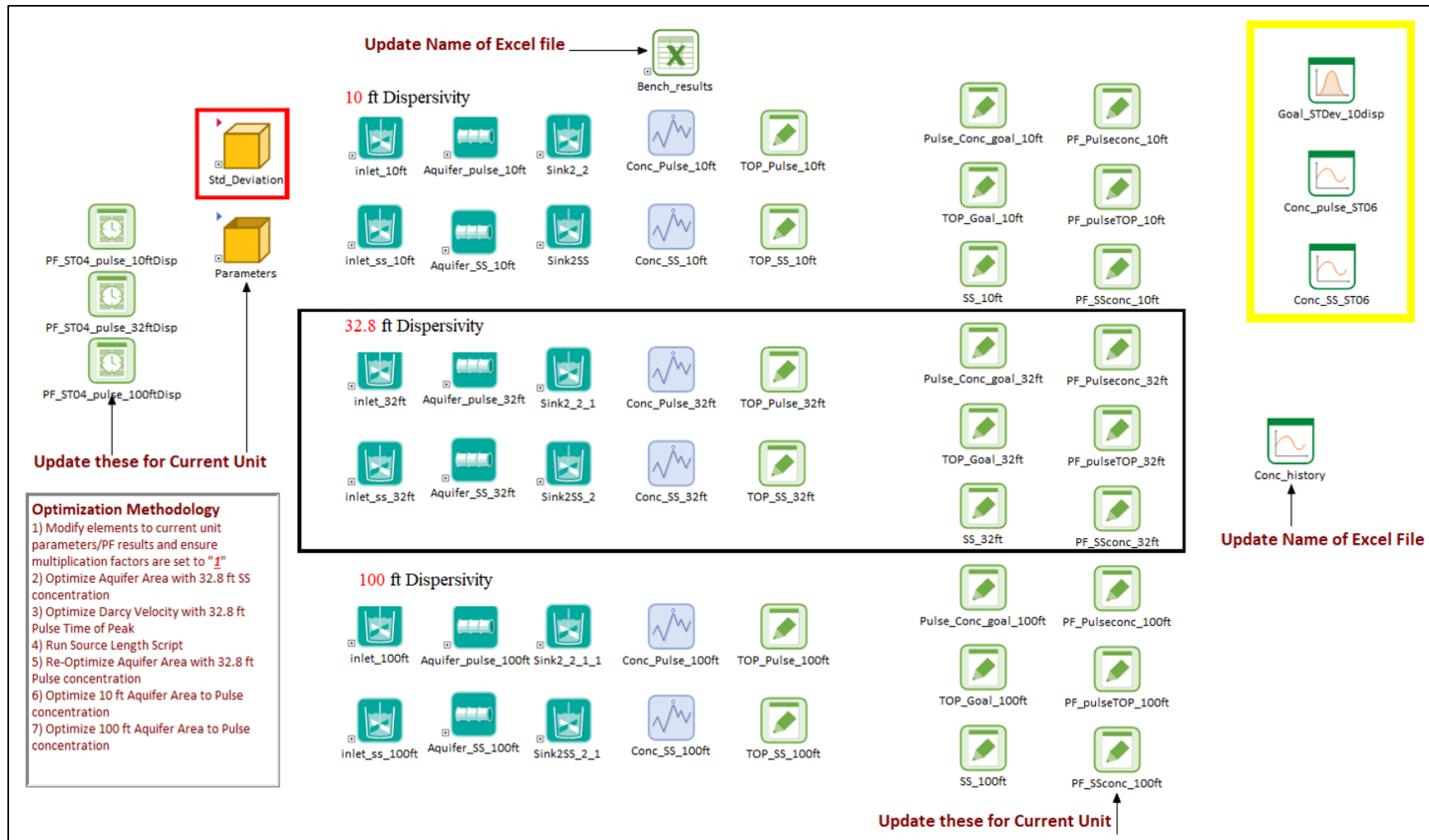


Figure 3-3. GoldSim® Aquifer Model template

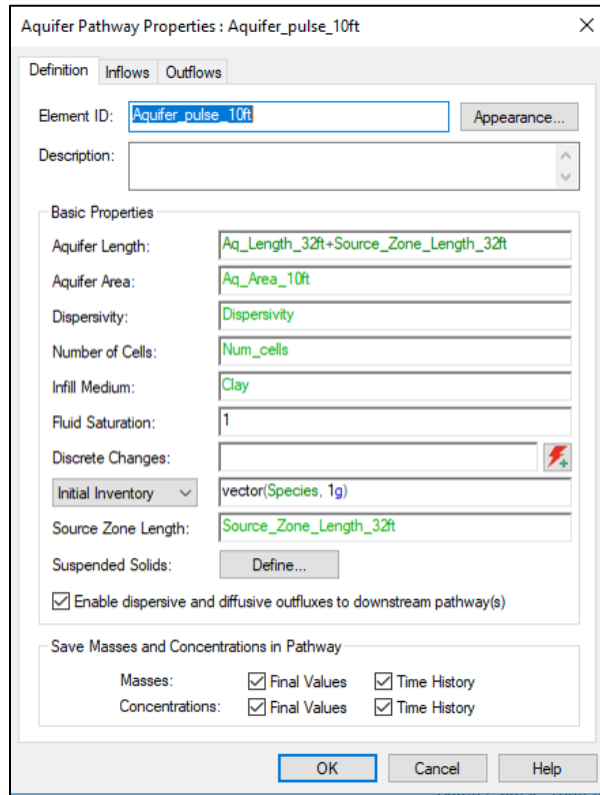


Figure 3-4. GoldSim® aquifer element illustrating some of the required geometric variables

The initial estimate for Darcy velocity is the ratio of the PF travel distance and arrival time, times effective porosity ($\eta_{\text{eff}} = 0.25$). The number of cells used to discretize the aquifer pathway controls numerical dispersion and thus affects pulse concentrations. The number of cells (Num_{cells}) was set to:

$$Num_{\text{cells}} = \text{round} \left[\frac{Aq_{\text{length}} + SourceZone_{\text{length}}}{Dispersivity} \cdot \frac{1}{2} \right] + 1 \quad (6)$$

so that numerical dispersion would approximately match the desired physical dispersion. Longitudinal dispersivity was set to zero.

Because *Dispersivity* is used to determine the number of cells, this parameter was not modified in the calibration procedure. PF travel distance was also kept fixed during model calibration. Calibration parameters include streamtube projected cross-sectional area (*Aq_Area*), Darcy velocity (*Darcy_vel*), and source zone length (*SourceZone_length*). Streamtube projected cross-sectional area affects the peak tracer concentration, Darcy velocity affects the plume arrival time, and the source zone length affects plume spread. Darcy velocity is particularly uncertain in the eastern section of E-Area because a portion of the tracer plume travels in the high-velocity TZ and the rest in the low-velocity TCCZ and LAZ. The effective source length is more uncertain for those DUs whose long axis is not aligned with the direction of flow. A schematic representation of the aquifer element is given in Figure 3-6. Aq_{length} in Equation 6 is represented by the blue-shaded area in Figure 3-6.

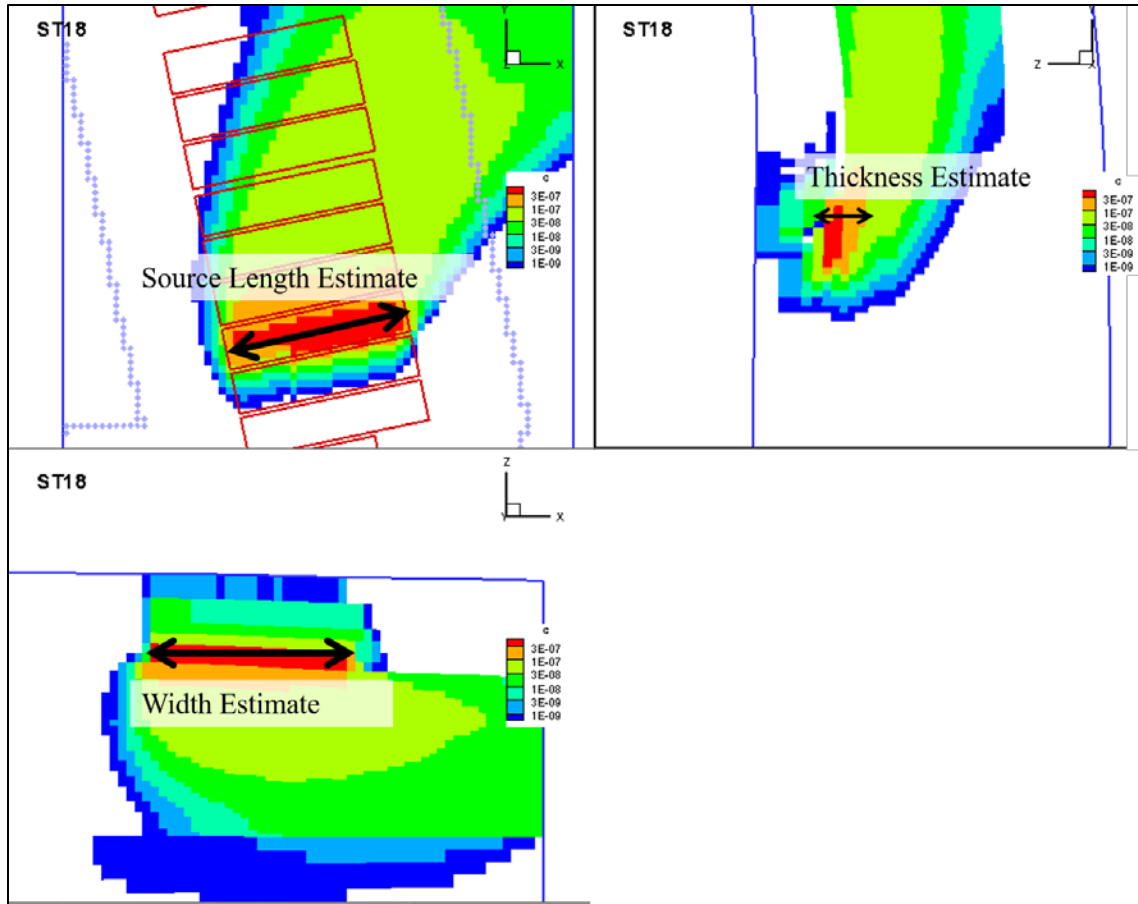


Figure 3-5. Teplot representation of the steady-state PORFLOW results utilized in estimating the source length and aquifer area *(Note the different views do not have the same magnification)

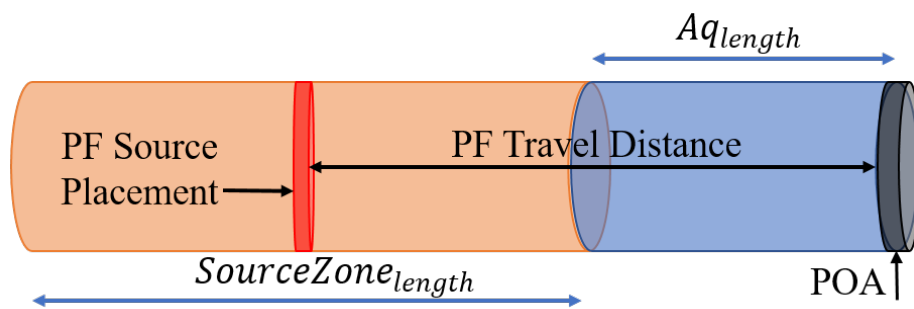


Figure 3-6. Schematic representation of the aquifer element

The initial estimates for the calibration parameters were placed in a separate subfolder, shown in Figure 3-7. Also noted in Figure 3-7 are the multipliers utilized in the calibration procedure discussed in Section 3.3. These data elements were then multiplied by the initial estimates to give the geometric parameters utilized in the aquifer element. This process is repeated for each of the 31 DUs studied in this report.

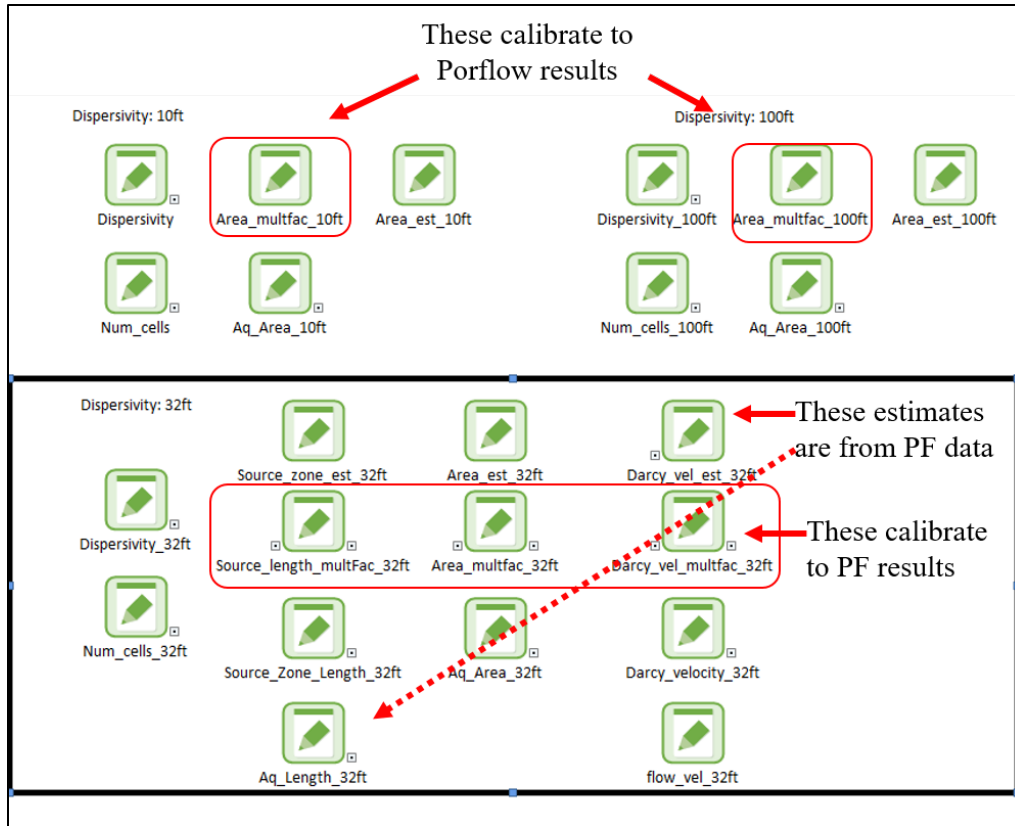


Figure 3-7. Parameter subfolder showing the variables utilized in the calibration procedure

3.3 Calibration

A total of six PF results were utilized in the calibration process: both a pulse and steady-state source at three different dispersivities. There were four different model output results to analyze for each DU: steady-state peak concentration, pulse peak concentration, pulse time-of-peak (TOP), and the pulse concentration profile shape. GS has a built-in optimization feature that minimizes the percent error of a result (objective function) by iteratively searching the solution space with different optimization variable values until convergence. The optimization screens displaying the optimization parameters are shown in Figure 3-8.

In this study, steady-state peak concentration, pulse peak concentration, and pulse TOP were optimized using this method where the objective function was the percent error of these results and the optimization variables were the aquifer area, Darcy velocity, and source-length multipliers. The optimization feature did not work well calibrating the source-length multiplier parameter to match plume spread; therefore, a script was created that performs separate GS simulations with a range of source-length multiplier values. The script opens the Aquifer Model and replaces the source-length multiplier element value as well as a book-keeping data element with the desired value. Within the script, this line is repeated several times using a range of source-length multiplier element values (from 0.20 to 1.58). The model utilizes a spreadsheet element to report the standard deviation (plume spread) and several other input and output data; the element is offset by the recordkeeping parameter to prevent overwriting. The proposed calibration flow diagram is given in Figure 3-9.

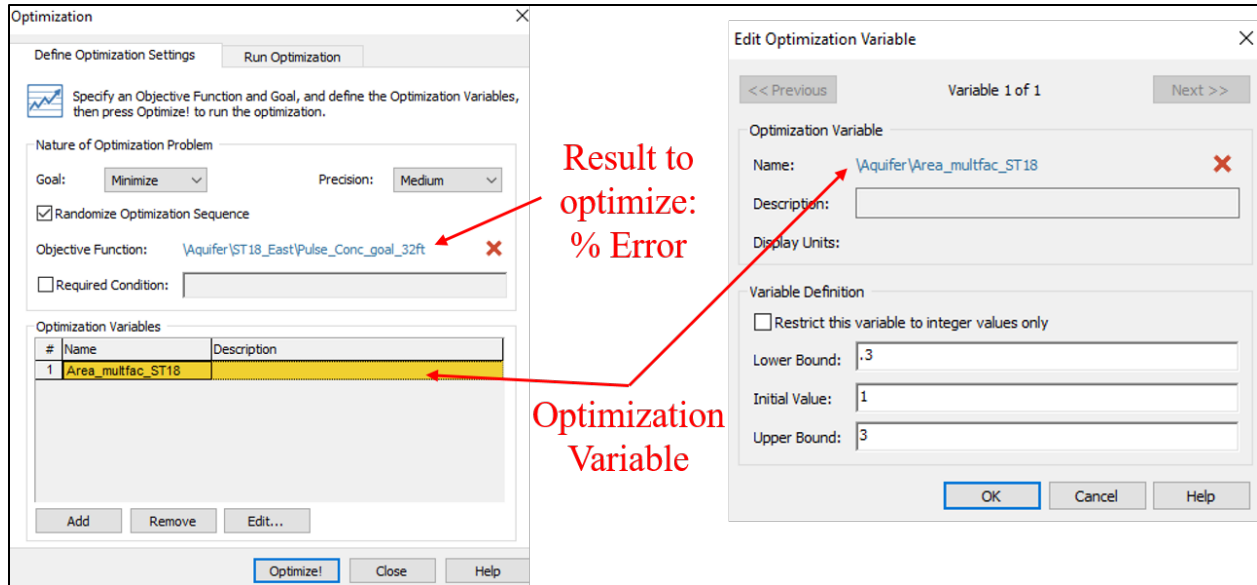


Figure 3-8. Optimization screens showing input parameters

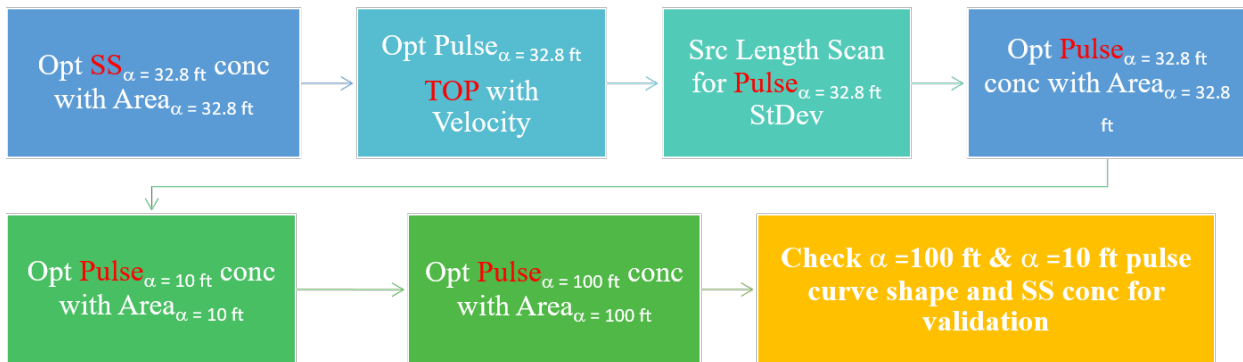


Figure 3-9. Calibration flow diagram

All multiplier elements were initially given a value of 1, so that the area, velocity, and source length were the estimated values obtained from the DU’s PF results. Utilizing GS’s optimization feature, the aquifer area is calibrated to minimize the error between the steady-state peak concentration predicted by GS and PF for the 32.8-foot dispersion tracer simulations. Applying the multiplier for aquifer area from the optimization routine, the Darcy velocity is calibrated next, minimizing the error between the TOP of the pulse simulation predicted by GS and PF. The shape of the pulse profile was found to be dependent on the source length, which was optimized by reducing the error in the standard deviation of the pulse concentration profile for the 32.8-foot dispersion case. For some DUs, this “simple” calibration procedure was adequate. In fact, a small subset of the DUs where the simple calibration procedure was adequate did

not even require the source-length scan to match the pulse concentration profile's standard deviation (i.e., source-length multiplier equal to 1.0). For example, see Figure 3-10.

On the other hand, for many DUs, the simple calibration procedure above produced 32.8-foot dispersivity pulse source results comparable to PF; however, the steady-state results were unacceptable. For these cases, multiple iterations of the optimization routine as well as manual calibration (i.e., visual check of peak shape and manual increase/decrease of variables) were required. An example of how manual calibration reduced the error in the GS results is shown in Figure 3-11.

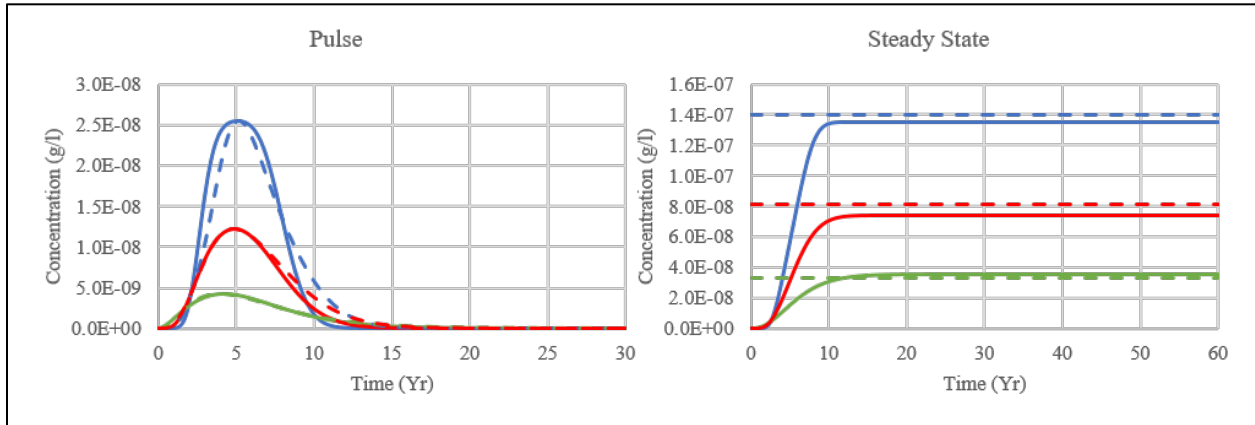


Figure 3-10. Example results from a successful “simple” calibration (dashed = PF, solid = GS)

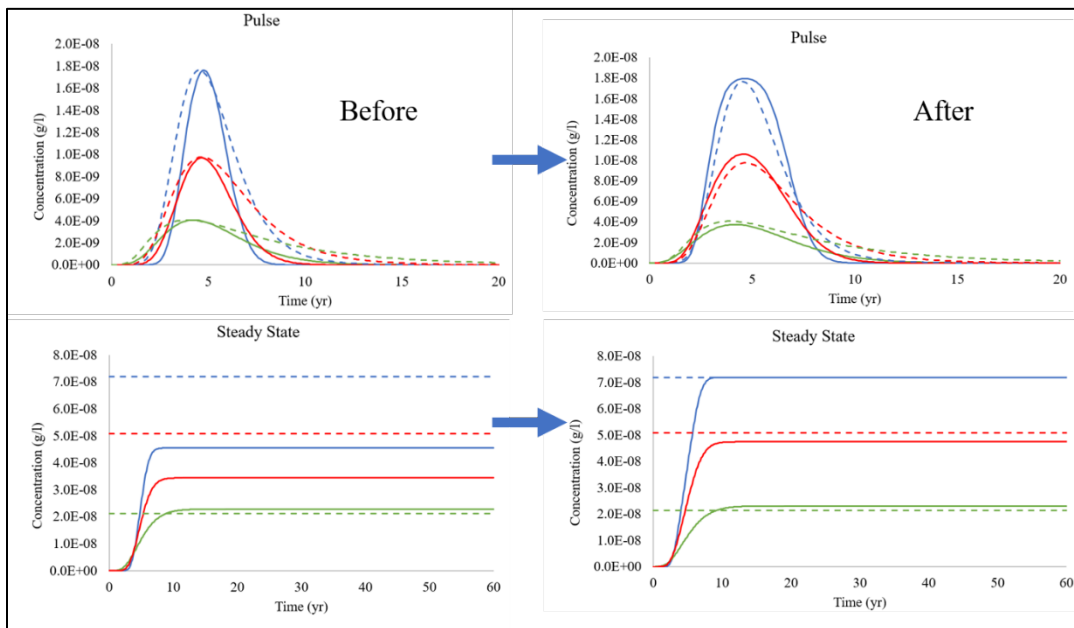


Figure 3-11. GS results showing concentration profiles before and after manual calibration

3.4 Plume Interaction

Because PAM is a one-dimensional representation of a three-dimensional transport process, the calculated solute concentrations include no spatial dispersion perpendicular to the direction of flow. In reality, radionuclide transport will disperse and may increase the solute concentrations at one or more neighboring DU's POA, as shown schematically in Figure 3-12. To calculate the contribution of solute mass from one DU (e.g., $Conc_C$ from unit C in Figure 3-12) to a neighboring POA, the GS Plume Function was initially considered. This analytic function is a built-in feature of GS and produces a multiplier applied to streamtube concentration to estimate concentrations off the streamtube centerline (Tauxe, 2014). In the context of Figure 3-12, the Plume Function can be used to estimate the concentrations at POA_A resulting from solute plumes emanating from DU sources B and C. However, the Plume Function requires several input parameters based on the geometry of the unit itself as well as the distances from the origin to the neighboring POAs. Upon testing, additional calibration was found to be required to match the PF results. To be more efficient, the decision was made to directly use the ratio of the PF contribution at the neighboring POA to the GS concentration at the origin POA as a correction factor. For example, the peak concentration generated by PF emanating from disposal unit C (Figure 3-12) at POA_A is divided by $Conc_C$ from GS to obtain the Plume Overlap Factor (POF).

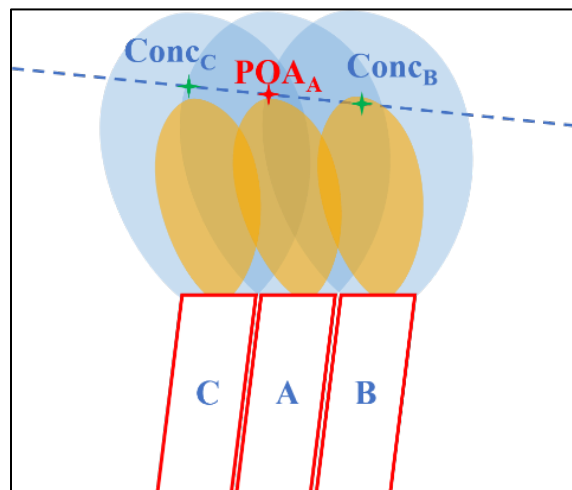


Figure 3-12. Schematic of plume interaction

4.0 Results

4.1 West Aquifer Model

Overall, the DUs in the West Aquifer Model required only simple calibration of the DUs and produced concentrations and time-of-peak values that were comparable to PF results. The relative ease of calibration is a result of the water table being located in the LAZ below the TCCZ, which avoids the plume being split by the TCCZ. Percent errors are listed in Table 4-1 while the optimized area, Darcy velocity, and source length are listed in Table 4-2.

Table 4-1. West Aquifer Model concentration and time-of-peak errors

$\alpha_L \rightarrow$	Steady-State Error			Pulse Error			Time-of-Peak Error		
	32.8 ft	10 ft	100 ft	32.8 ft	10 ft	100 ft	32.8 ft	10 ft	100 ft
DU8A	0%	6%	1%	2%	0%	0%	0%	0%	3%
DU8B	0%	3%	6%	4%	0%	2%	0%	6%	4%
DU8C	0%	5%	0%	7%	2%	5%	4%	3%	5%
ET03	6%	10%	5%	3%	17%	4%	0%	0%	9%
ET04	10%	5%	10%	0%	0%	0%	2%	15%	0%
ILV	0%	10%	12%	3%	11%	0%	0%	1%	0%
NRCDA26E	8%	16%	8%	2%	14%	4%	0%	1%	0%
ST08	9%	3%	7%	0%	0%	0%	0%	2%	5%
ST09	0%	14%	12%	2%	0%	0%	0%	4%	5%
ST10	13%	13%	16%	0%	0%	0%	0%	13%	30%

Table 4-2. Calibrated West Aquifer Model geometric parameter multiplier values

	Final Area $\alpha_L = 32.8$ ft (m ²)	Final Area $\alpha_L = 10$ ft (m ²)	Final Area $\alpha_L = 100$ ft (m ²)	Darcy Velocity Multiplier	Source-Length Multiplier
DU8A	1189	585	2326	1.26	1.00
DU8B	1225	686	2333	1.38	1.00
DU8C	1706	975	2747	1.10	0.80
ET03	2689	1656	4568	1.10	1.35
ET04	2513	1624	5326	1.01	1.58
ILV	2569	1696	4619	0.90	1.00
NRCDA26E	2004	1303	3719	1.01	1.15
ST08	1430	775	2972	0.94	1.00
ST09	1395	710	2979	0.88	1.00
ST10	1433	870	2499	0.87	1.00

4.1.1 Disposal Units 8A, 8B, & 8C

Figure 4-1 compares the GS DU 8A, 8B, and 8C POA concentrations for steady-state and pulse sources to the PF results. DU 8A and 8B required the simple calibration only, whereas calibration of DU 8C needed additional adjustment of the source-length and area multipliers to reduce the errors observed between the PF and GS steady-state results. The final calibrations produced small errors (less than 10%) for each case.

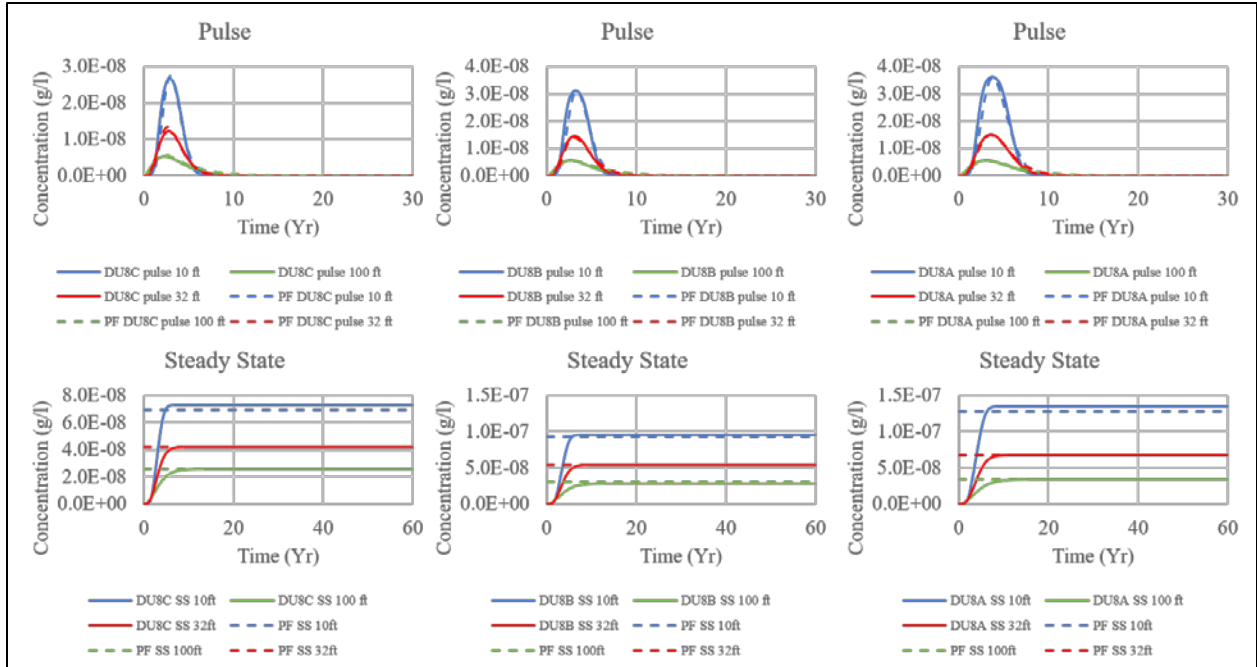


Figure 4-1. GS POA concentrations for DU 8A-C compared to PF results

4.1.2 West Engineered Trenches

Figure 4-2 compares the GS Engineered Trench (ET) 3 and 4 POA concentrations for steady-state and pulse sources to PF results. ET 4 required the simple calibration only whereas calibration of ET 3 needed additional adjustment of the source-length and area multipliers to reduce the errors observed between the PF and GS steady-state and pulse source displays. Interestingly, the pulse source concentration profile for the PF 10-foot dispersivity tracer case displays a ‘shoulder’ that appears after the initial breakthrough. The shoulder could result from the water table passing partially through the TCCZ. The final calibrations produced small errors ($\leq 10\%$) for all other results.

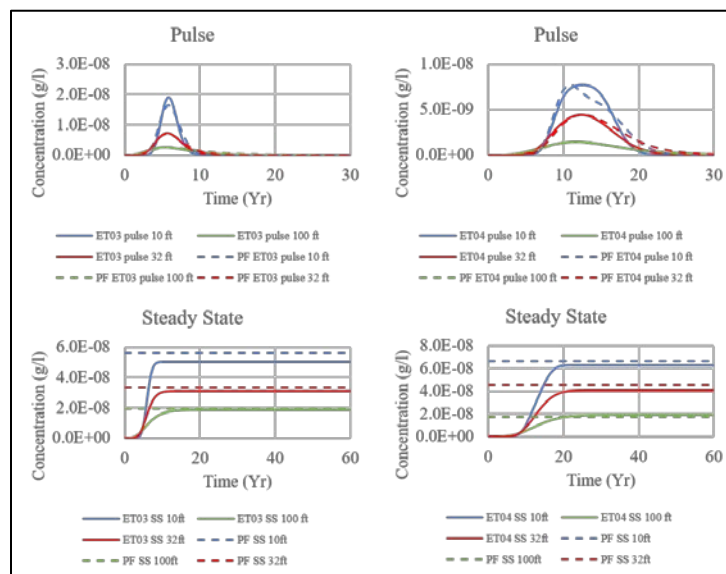


Figure 4-2. GS POA concentrations for ET 3 and 4 compared to PF results

4.1.3 Intermediate Level Vault & Naval Reactor Component Disposal Area

Figure 4-3 compares the GS Intermediate Level Vault (ILV) and Naval Reactor Component Disposal Area (NRCDA) 26E POA concentrations for steady-state and pulse sources to the PF results. The ILV required the simple calibration with no source-length correction (source-length multiplier equals 1.0) because the shape of the pulse concentration profile matched the PF results well using the uncorrected source-length estimate value. NRCDA 26E, on the other hand, needed additional adjustment of both the source-length and area multipliers to reduce the errors observed between the PF and GS steady-state source results.

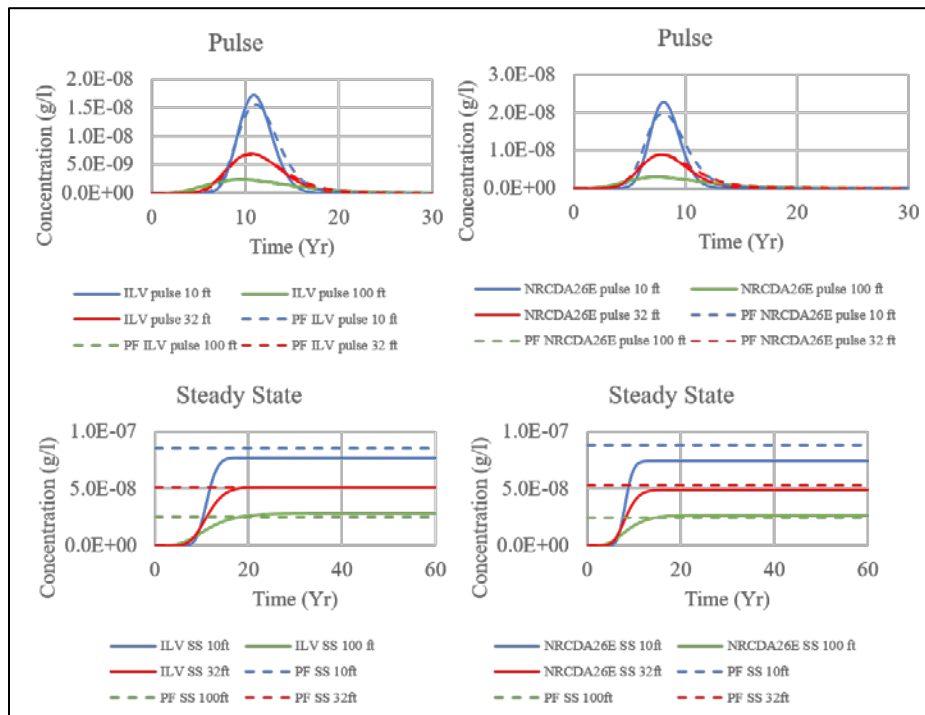


Figure 4-3. GS POA concentrations for ILV and NRCDA 26E compared to PF results

4.1.4 West Slit Trenches

Figure 4-4 compares POA concentrations for GS Slit Trenches (ST) 8, 9, and 10 to the PF results for steady-state and pulse sources. There was good agreement in the shapes of the concentration profiles for the GS and PF pulse-source simulations for all West ST models when using the initial source-length estimate value; therefore, only the simple calibration without source-length modification was required. Like ET 4, the ST 10 PF pulse-source tracer results display a ‘shoulder’ that appears during the initial breakthrough for both the 10-foot and 32.8-foot dispersivity cases. Again, the shoulder can be attributed to the water table passing partially through the TCCZ and is the source of the somewhat larger (13-30%) errors observed for this disposal unit.

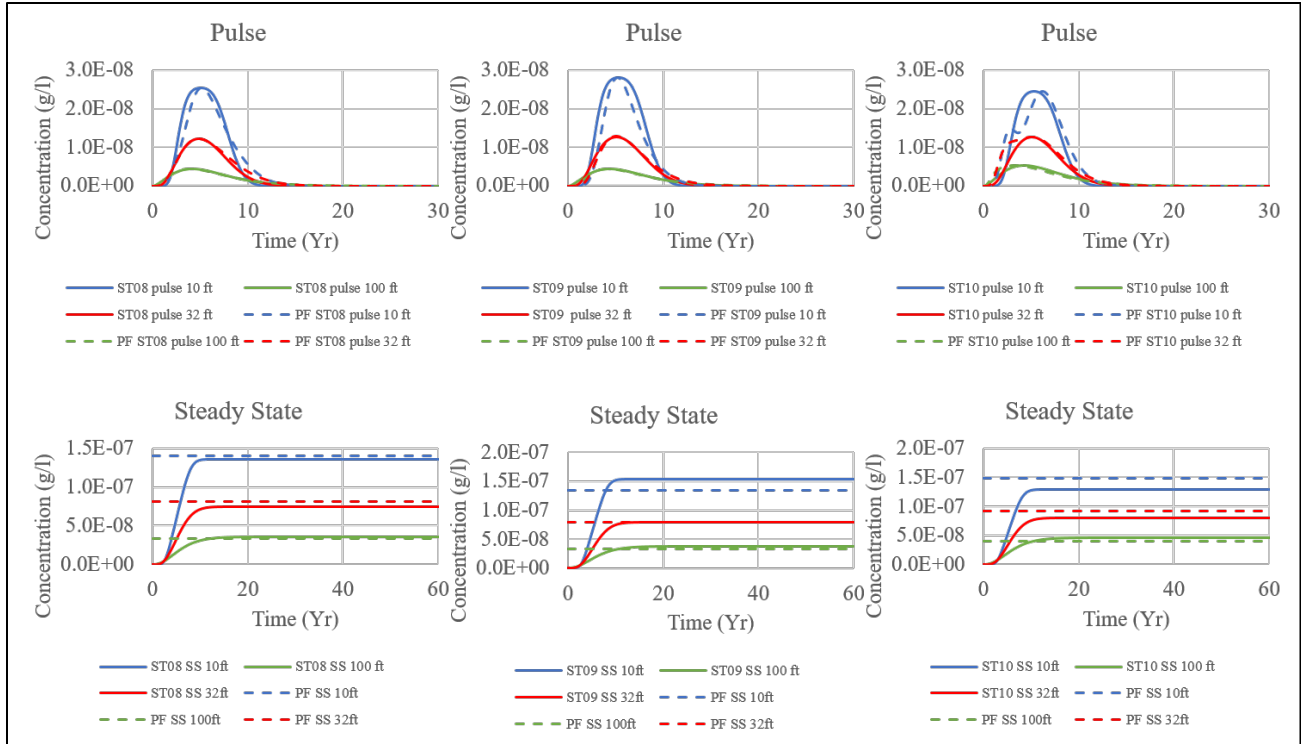


Figure 4-4. GS POA concentrations for ST 8-10 compared to PF results

4.2 Center Aquifer Model

The center ST DUs required only simple calibration with no modifications to the initial PF source-length estimates. The Components-in-Grout (CIG) trenches, on the other hand, required additional calibration, including manual manipulation of both the area and source-length multipliers to better match PF results. The percent errors are listed in Table 4-3 and the optimized area, Darcy velocity multiplier, and source-length multiplier are listed in Table 4-4.

Table 4-3. Center Aquifer Model concentration and time-of-peak errors

$\alpha_L \rightarrow$	Steady-State Error in Peak Concentration			Pulse Error in Peak Concentration			Time-of-Peak Error		
	32.8 ft	10 ft	100 ft	32.8 ft	10 ft	100 ft	32.8 ft	10 ft	100 ft
ST01	0%	4%	22%	2%	0%	0%	0%	1%	10%
ST02	0%	1%	19%	1%	0%	0%	0%	2%	8%
ST03	0%	5%	18%	3%	0%	0%	0%	2%	8%
ST04	0%	12%	19%	6%	0%	0%	0%	3%	10%
ST11	0%	2%	22%	7%	0%	0%	0%	3%	8%
CIG1	0%	0%	1%	0%	5%	22%	3%	3%	44%
CIG2	0%	9%	14%	0%	0%	17%	3%	6%	59%

Table 4-4. Calibrated Center Aquifer Model geometric parameter multiplier values

	Final Area $\alpha_L = 32.8$ ft (m²)	Final Area $\alpha_L = 10$ ft (m²)	Final Area $\alpha_L = 100$ ft (m²)	Darcy Multiplier	Source-Length Multiplier
ST01	1592	947	2835	1.00	1.00
ST02	1422	867	2633	1.22	1.00
ST03	1399	927	2588	1.29	1.00
ST04	1390	1013	2518	1.28	1.00
ST11	1655	985	3073	0.85	1.00
CIG1	1482	962	3230	1.12	0.87
CIG2	1480	1065	2886	1.16	0.75

4.2.1 Center Slit Trenches

Figure 4-5 compares the GS center ST (ST 1, 2, 3, 4 and 11) POA concentrations for steady-state and pulse sources to the PF results. The center ST DUs required only the simple calibration with no modifications to the initial PF source-length estimates; pulse and time-of-peak results were excellent ($\leq 10\%$). The 100-foot dispersivity steady-state simulations resulted in larger errors (18-22%), but are still acceptable.

4.2.2 Components-in-Grout Trenches

POA concentration profiles from the GS and PF simulations for CIG 1 and 2 steady-state and pulse sources are compared in Figure 4-6. CIG 1 required the simple calibration only, but with source-length calibration. CIG 2 needed additional manual adjustment of the source-length and area multipliers to reduce the errors observed between the PF and GS steady-state and pulse source simulations. While the CIG DUs 32.8-foot and 10-foot dispersivity simulations produced errors less than 10%, the 100-foot pulse simulations produced TOP errors larger than 20% and the peak concentration errors ranged from 17-22%.

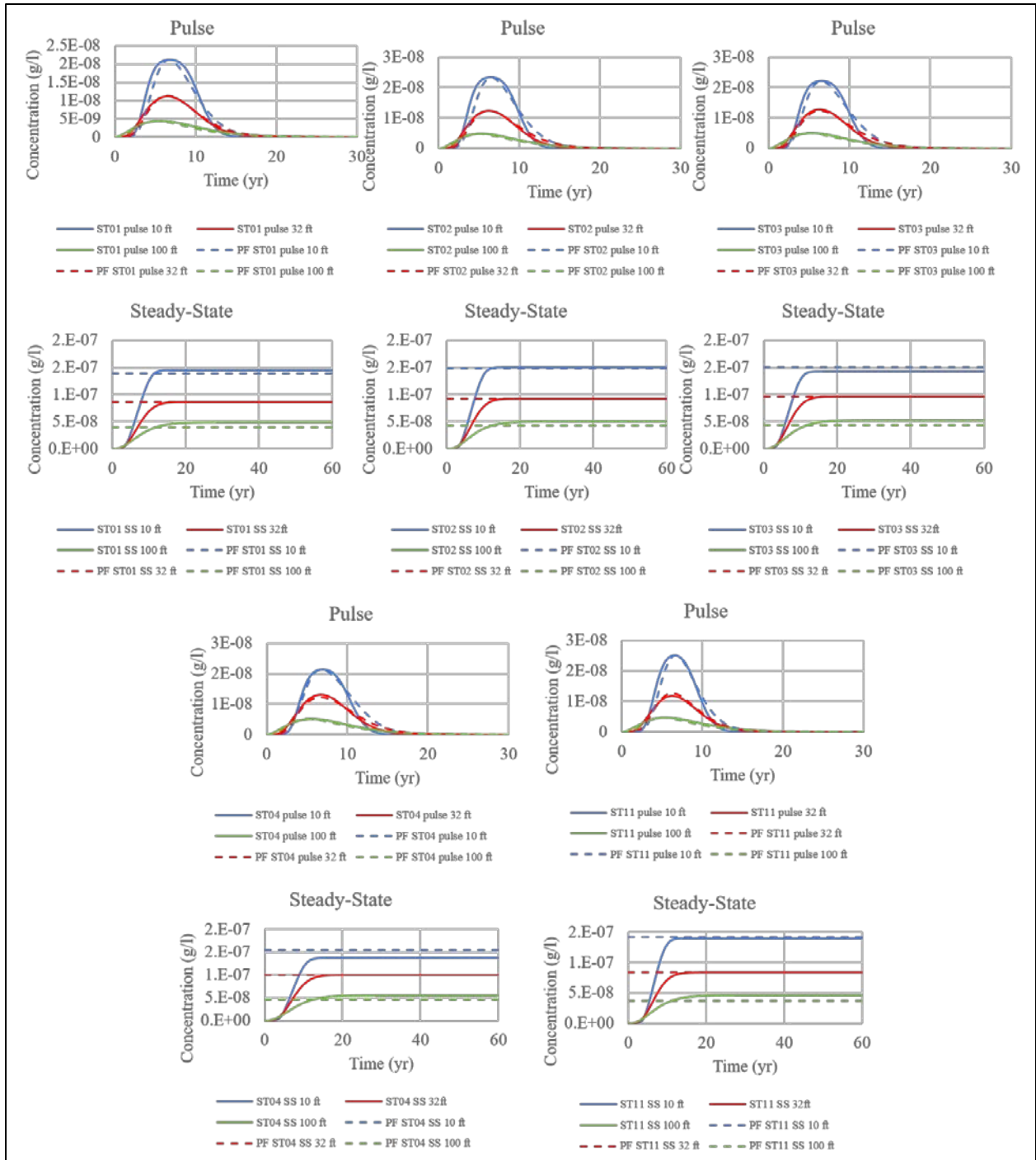


Figure 4-5. GS POA concentrations for ST 1-4 & 11 compared to PF results

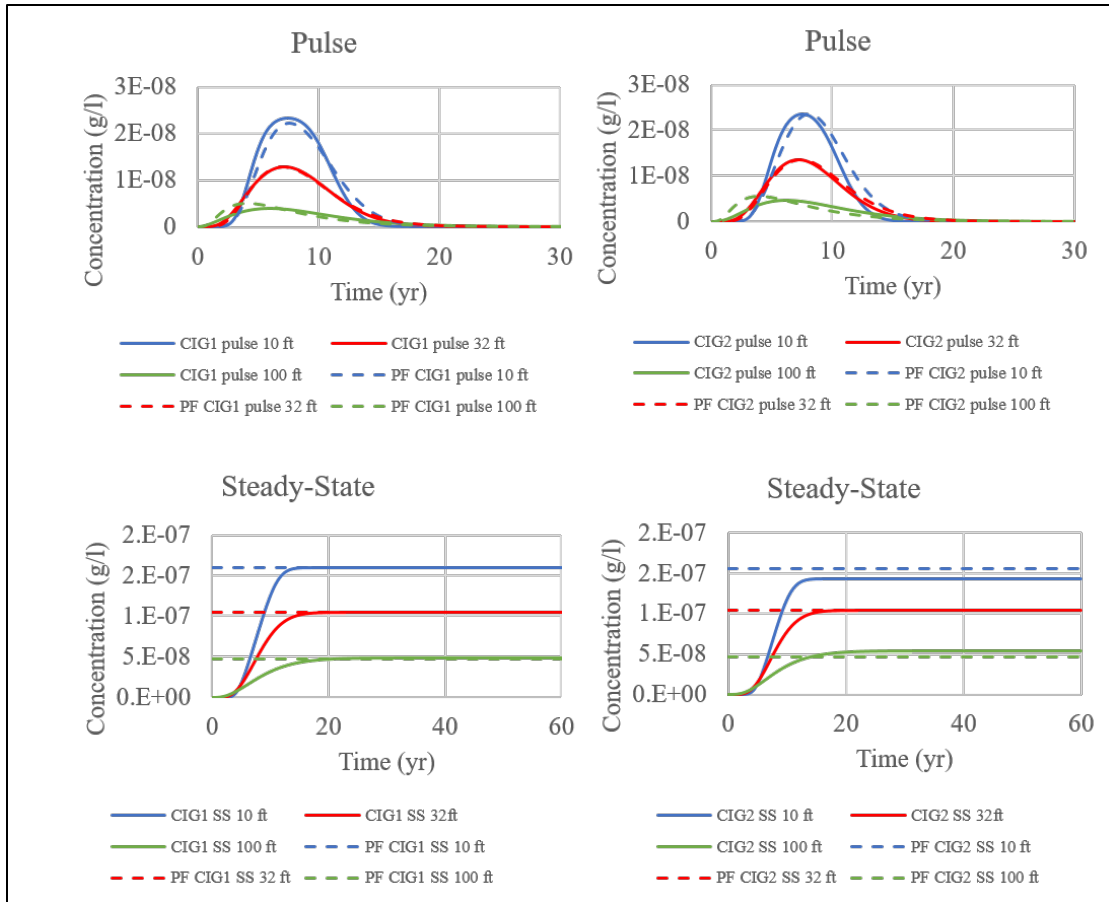


Figure 4-6. GS POA concentrations for CIG 1 & 2 compared to PF results

4.3 East Aquifer Model

All East DUs required additional calibration, including manual manipulation of both the area and source-length multipliers, to better match the PF results. This is likely due to the plume traveling partially in the high-velocity TZ and the low-velocity TCCZ and LAZ, as well as the streamtraces not being oriented perpendicular to the DU's cross-section. The percent errors are listed in Table 4-5 and the optimized area, Darcy velocity multiplier, and source-length multiplier are listed in Table 4-6.

4.3.1 East Slit Trenches

Figure 4-7 and Figure 4-8 compare the GS East ST's POA concentration profiles for steady-state and pulse sources to the PF results. Most East ST simulation results are comparable to PF's with errors less than 20%. More specifically, all 32.8-foot dispersivity cases have errors less than 15%, while errors in peak concentration for ST 5, 6, and 7 assuming a 100-foot dispersivity were greater than 20% (e.g., the ST 5 error for a steady-state source with 100-foot dispersivity was 124% with the next largest error being 35%). It should be noted that ST 21's aquifer length is exceptionally long, approximately 600 meters. For the 10-foot dispersivity case, 114 cells were needed for an accurate representation of dispersivity. Because the GS aquifer element comprises a maximum of only 100 cells, this introduces another source of error.

Table 4-5. East Aquifer Model concentration and time-of-peak errors

$\alpha_L \rightarrow$	Steady-State Error			Pulse Error			Time-of-Peak Error		
	32 ft	10 ft	100 ft	32 ft	10 ft	100 ft	32.8 ft	10 ft	100 ft
ST05	3%	5%	124%	4%	2%	23%	0%	4%	81%
ST06	11%	0%	20%	5%	0%	27%	0%	18%	3%
ST07	11%	1%	35%	4%	4%	20%	3%	18%	3%
ST14	3%	11%	18%	0%	3%	9%	2%	2%	16%
ST15	8%	10%	17%	1%	0%	0%	3%	7%	3%
ST16	5%	0%	24%	0%	0%	12%	1%	5%	7%
ST17	0%	0%	17%	8%	6%	12%	0%	0%	8%
ST18	10%	0%	14%	0%	11%	12%	1%	4%	13%
ST19	4%	1%	16%	0%	0%	10%	0%	4%	11%
ST20	0%	14%	14%	0%	0%	5%	1%	2%	4%
ST21	13%	9%	19%	10%	3%	0%	0%	0%	7%
ET1	7%	0%	9%	9%	2%	8%	2%	2%	8%
ET2	8%	2%	15%	7%	2%	0%	0%	3%	13%
LAWV	14%	4%	12%	0%	1%	5%	2%	2%	4%

Table 4-6. Calibrated East Aquifer Model geometric parameter multiplier values

	Final Area $\alpha_L = 32.8$ ft (m ²)	Final Area $\alpha_L = 10$ ft (m ²)	Final Area $\alpha_L = 100$ ft (m ²)	Darcy Multiplier	Source-Length Multiplier
ST05	1550	1007	2790	1.08	0.80
ST06	951	608	2377	2.43	1.15
ST07	962	601	2116	2.48	1.10
ST14	1099	720	2369	3.53	1.31
ST15	1003	619	2062	3.65	1.58
ST16	1622	1165	3325	2.43	1.30
ST17	1825	1347	4105	2.22	1.15
ST18	2012	1300	4098	2.41	1.18
ST19	2030	1315	4162	2.43	1.38
ST20	2184	1259	4413	2.47	1.58
ST21	5054	3469	9143	1.12	1.35
ET01	1236	808	2540	2.95	1.33
ET02	1135	717	1987	3.12	1.16
LAWV	1349	902	2834	2.97	1.28

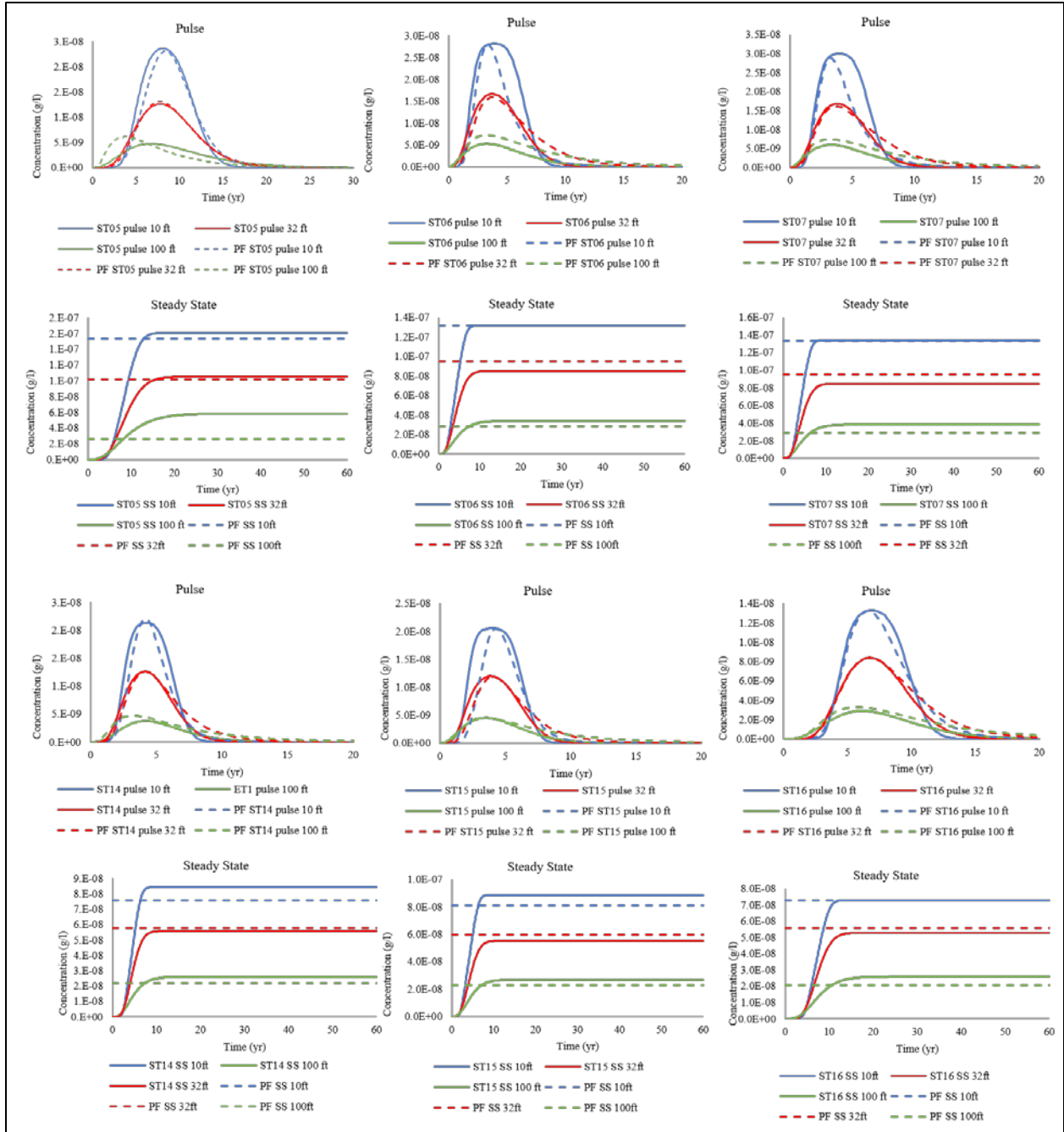


Figure 4-7. GS POA concentrations for ST 5, 6, 7, 14 and 16 compared to PF results

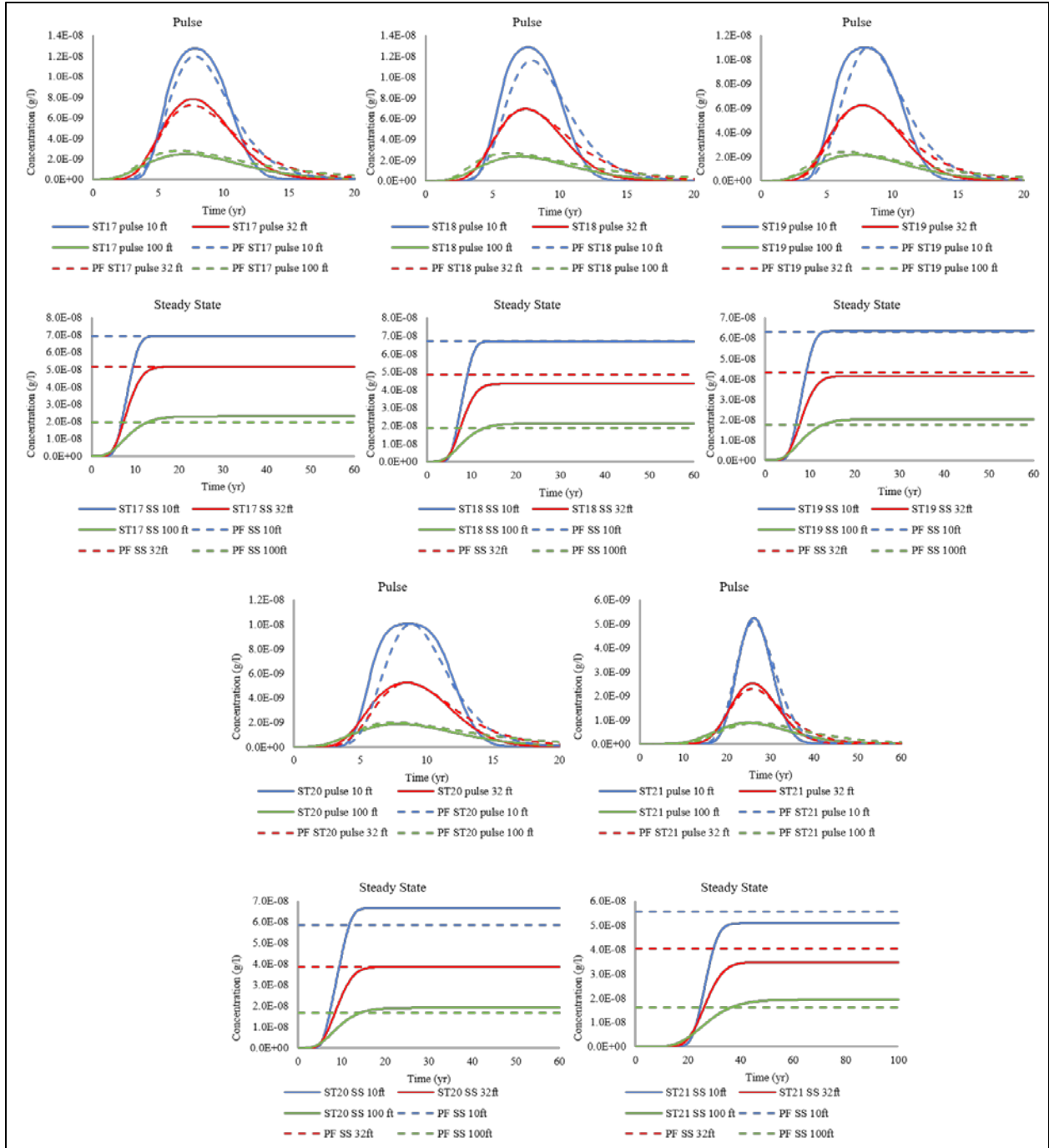


Figure 4-8. GS POA concentrations for ST 17, 18, 19, 20, and 21 compared to PF results

4.3.2 East Engineered Trenches and Low-Activity Waste Vault

GS-predicted POA concentrations for steady-state and pulse sources for the GS East ETs and Low-Activity Waste Vault (LAWV) are compared to PF results in Figure 4-9. All units required additional modification of the multiplication data elements to reduce the steady-state concentration errors. After final calibration, the maximum error for these units was 15%.

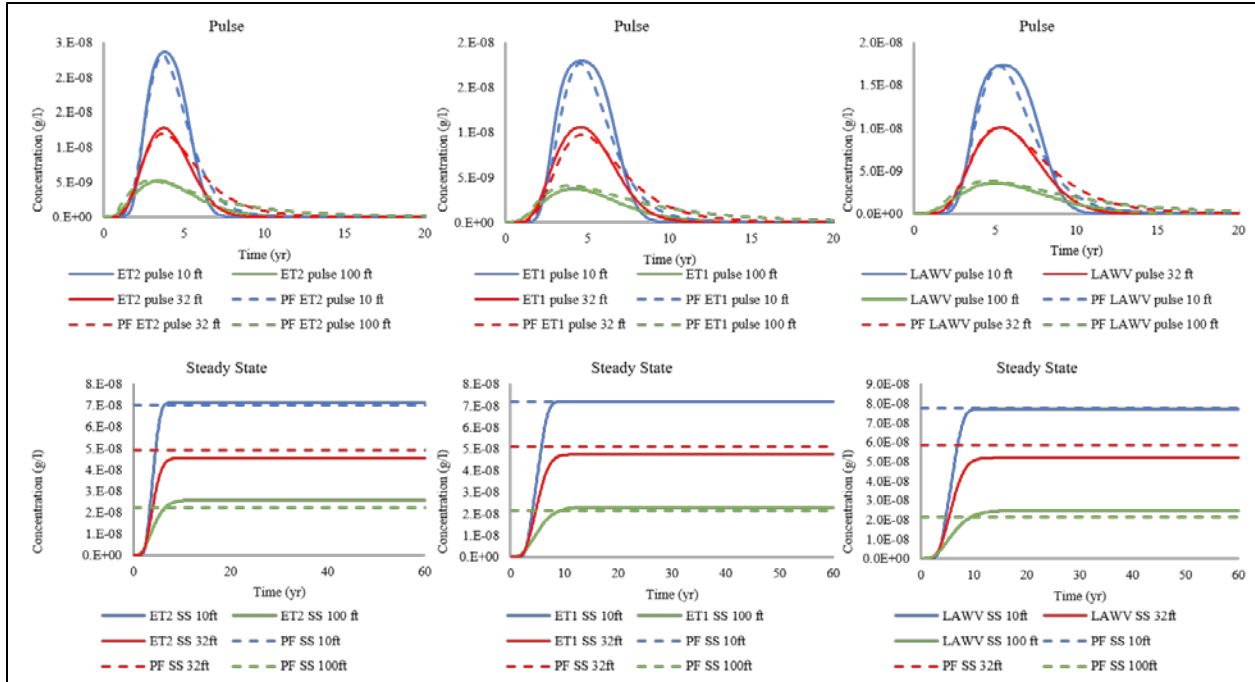


Figure 4-9. GS POA concentrations for ET 1 & 2 and LAWV compared to PF results

4.4 Plume Overlap Factors

The steady-state source plume overlap factors (POF) are derived in this section for each PAM submodel (i.e., disposal unit) as well as for the overlap from DUs located in neighboring models (i.e., East, Central, and West). Ideally, the steady-state and pulse sources would have very similar POFs as only one overlap factor will be utilized in the GS system model. Unfortunately, for many DUs, the steady-state POFs were larger/smaller than the corresponding pulse POFs. In the ELLWF system model, PAM’s input will be mass flux at the water table. Because many of the radionuclides produce long-lasting fluxes (as opposed to peaking and falling to zero within the simulation time) and most of the steady-state POFs are greater than POFs for their pulse counterparts, the steady-state POF results were chosen for presentation in this report. The pulse POFs are summarized in Appendix A. Note that only POFs larger than or equal to 0.01 are listed in the tables.

Plume overlap factors from neighboring models (e.g., the contribution of ST11 from the Center Aquifer Model to ST10 in the West Aquifer Model) were calculated from the PF concentration contribution results taken from the aquifer model where the POA is located. For example, the ST11 concentration contribution to the ST10 POA concentration is taken from the west PF tracer simulations because the ST10 POA lies near the boundary with the Center Aquifer Model where ST11 is located (as seen in Figure 2-1).

4.4.1 West Aquifer Model

The West Aquifer Model’s POFs for the steady-state source 32.8-foot, 10-foot, and 100-foot dispersivity simulations are listed in Table 4-7, Table 4-8, and Table 4-9, respectively. As expected, the factors are larger where the streamtraces (Figure 2-1) for neighboring DUs are in close proximity. The largest POF is the contribution of NRCDA 26E to the centerline POA of ET03 and vice versa. Note that these POFs exceed 1.00, because GS underestimates the centerline POA concentrations for these units. The contributions of

ILV and ST09 to each other are also large (0.75/0.70). Only two DUs from the Center Aquifer Model contribute to West Aquifer Model POAs: ST11 and ST01. The largest contribution for the 32.8-foot dispersivity, steady-state case was from ST11, which contributes 0.10 times its centerline POA concentration to ST10.

Table 4-7. West Aquifer Model’s plume overlap factors: 32.8-foot dispersivity, steady-state source

DU→ POA↓	ST08	ST09	ST10	ET03	ET04	ILV	NRCDA 26E	DU8A	DU8B	DU8C	ST11 Center	ST01 Center
ST08		0.26	0.02			0.32	0.02					
ST09	0.18		0.19			0.75					0.01	
ST10		0.20				0.43					0.10	0.01
ET03	0.08	0.02			0.07	0.03	1.02			0.02		
ET04				0.75			0.07		0.02	0.42		
ILV	0.08	0.70	0.24								0.01	
NRCDA 26E	0.06	0.01		1.01	0.08	0.03				0.01		
DU8A												
DU8B					0.03			0.10				
DU8C	0.01			0.13	0.34		0.02		0.19			

Table 4-8. West Aquifer Model’s plume overlap factors: 10-foot dispersivity, steady-state source

DU→ POA↓	ST08	ST09	ST10	ET03	ET04	ILV	NRCDA 26E	DU8A	DU8B	DU8C	ST11 Center
ST08		0.08		0.01		0.21	0.03				
ST09	0.21		0.08			0.54					
ST10		0.21				0.33					0.02
ET03	0.01				0.09		1.15			0.01	
ET04				0.53			0.04		0.01	0.08	
ILV	0.09	0.46	0.09								
NRCDA 26E	0.01			0.81	0.10						
DU8A											
DU8B								0.06			
DU8C				0.04	0.10				0.12		

Table 4-9. West Aquifer Model’s plume overlap factors: 100-foot dispersivity, steady-state source

DU→ POA↓	ST08	ST09	ST10	ET03	ET04	ILV	NRCDA 26E	DU8A	DU8B	DU8C	ST11 Center	ST01 Center
ST08		0.57	0.12	0.09	0.01	0.56	0.14				0.02	
ST09	0.33		0.42	0.01		0.74	0.01				0.07	0.01
ST10	0.05	0.35				0.46					0.26	0.03
ET03	0.27	0.11	0.03		0.26	0.14	0.82			0.10		
ET04	0.06	0.02	0.01	0.78		0.03	0.32		0.09	0.77		
ILV	0.24	0.76	0.48				0.01				0.07	0.01
NRCDA 26E	0.26	0.10	0.02	0.96	0.29	0.14				0.09		
DU8A					0.01				0.02			
DU8B				0.04	0.21		0.02	0.21		0.03		

DU8C	0.04	0.02		0.36	0.60	0.02	0.14	0.00	0.31			
------	------	------	--	------	------	------	------	------	------	--	--	--

4.4.2 Center Aquifer Model

The Center Aquifer Model’s POFs for the steady-state source 32.8-foot, 10-foot, and 100-foot dispersivity simulations are listed in Table 4-10, Table 4-11, and Table 4-12, respectively. The POFs for the Center Aquifer Model DUs are smaller than those for the West and East Aquifer Models. This is expected because the streamtraces are more distant from each other and have little overlap. The largest POF is the contribution of ST01 to the centerline POA of ST11 (POF = 0.27). Although four West Aquifer Model DUs are predicted to contribute to ST11, CIG1 and CIG2, only the contribution from ST05 to CIG2’s centerline POA has a POF at or above 0.01 for both the 32.8-foot and 10-foot dispersivity cases.

Table 4-10. Center Aquifer Model’s plume overlap factors: 32.8-foot dispersivity, steady-state source

DU→ POA↓	ST01	ST02	ST03	ST04	ST11	CIG1	CIG2	ST10 West	ILV West	ST05 East	ST06 East
ST01		0.24			0.15						
ST02	0.13		0.24								
ST03		0.11		0.19							
ST04			0.12			0.14					
ST11	0.27	0.01									
CIG1				0.10			0.13				
CIG2						0.12				0.12	

Table 4-11. Center Aquifer Model’s plume overlap factors: 10-foot dispersivity, steady-state source

DU→ POA↓	ST01	ST02	ST03	ST04	ST11	CIG1	CIG2	ST10 West	ILV West	ST05 East	ST06 East
ST01		0.17			0.18						
ST02	0.14		0.18								
ST03		0.13		0.17							
ST04			0.16			0.13					
ST11	0.15										
CIG1				0.14			0.13				
CIG2						0.15				0.12	

Table 4-12. Center Aquifer Model’s plume overlap factors: 100-foot dispersivity, steady-state source

DU→ POA↓	ST01	ST02	ST03	ST04	ST11	CIG1	CIG2	ST10 West	ILV West	ST05 East	ST06 East
ST01		0.42	0.07		0.29						
ST02	0.28		0.42	0.06	0.02						
ST03	0.02	0.28		0.37		0.05					
ST04		0.02	0.29			0.36	0.03				
ST11	0.47	0.10	0.01					0.01	0.04		

CIG1			0.02	0.27			0.32			0.03	
CIG2				0.02		0.36				0.29	0.05

4.4.3 East Aquifer Model

The East Aquifer Model’s POFs for the steady-state source 32.8-foot, 10-foot, and 100-foot dispersivity simulations are listed in Table 4-13, Table 4-14, and Table 4-15, respectively. As expected, ST05, ST06, and ST07 have relatively small POFs because their streamtraces are separated when compared to other DUs in the East Aquifer Model. Compared to the West and Center Aquifer Models, the East Aquifer Model has consistently larger POFs with 22 factors exceeding 0.50 for the 32.8-foot dispersivity, steady-state simulations. The largest POF (0.97) is for the contribution of LAWV to the centerline POA for ST15. In most cases, the larger POFs (0.80 and above) arise because of mass contributions of the more southern DUs (from LAWV to ST20) to the DU plume of interest located immediately to the north.

Table 4-13. East Aquifer Model’s plume overlap factors: 32.8-foot dispersivity, steady-state source

DU→ POA↓	ST 05	ST 06	ST 07	ST 14	ST 15	ST 16	ST 17	ST 18	ST 19	ST 20	ST 21	ET 01	ET 02	LAWV	CIG2 Center
ST05		0.15													0.12
ST06	0.04		0.10										0.06		
ST07		0.15										0.03	0.19		
ST14					0.84	0.27	0.15	0.08	0.04	0.02	0.01	0.20		0.52	
ST15				0.16		0.57	0.34	0.24	0.13	0.08	0.04			0.97	
ST16					0.02		0.81	0.65	0.42	0.26	0.16			0.65	
ST17						0.72		0.91	0.62	0.40	0.27			0.09	
ST18						0.05	0.57		0.96	0.69	0.40				
ST19							0.10	0.65		0.92	0.31				
ST20							0.03	0.43	0.95		0.25				
ST21					0.01	0.17	0.28	0.47	0.58	0.68				0.08	
ET01				0.67	0.41	0.09	0.04	0.01	0.01				0.06	0.22	
ET02				0.31	0.17	0.01						0.64		0.05	
LAWV					0.47	0.81	0.52	0.39	0.24	0.14	0.08				

Table 4-14. East Aquifer Model’s plume overlap factors: 10-foot dispersivity, steady-state source

DU→ POA↓	ST 05	ST 06	ST 07	ST 14	ST 15	ST 16	ST 17	ST 18	ST 19	ST 20	ST 21	ET 01	ET 02	LAWV	CIG2 Center
ST05		0.16													0.16
ST06	0.03		0.07										0.01		
ST07		0.13										0.01	0.05		
ST14					0.76	0.24	0.10	0.04	0.01			0.22		0.49	
ST15				0.11		0.61	0.33	0.16	0.06	0.02	0.01			0.96	
ST16					0.01		0.90	0.62	0.34	0.14	0.06			0.45	
ST17						0.55		0.89	0.58	0.28	0.14			0.05	
ST18						0.03	0.44		0.94	0.59	0.29				
ST19							0.07	0.49		0.81	0.24				
ST20							0.02	0.29	0.82		0.20				
ST21						0.02	0.07	0.18	0.34	0.46					
ET01				0.57	0.34	0.05	0.02						0.09	0.15	
ET02				0.18	0.10	0.01						0.43		0.03	
LAWV					0.30	0.88	0.57	0.32	0.14	0.05	0.02				

Table 4-15. East Aquifer Model’s plume overlap factors: 100-foot dispersivity, steady-state source

DU→ POA↓	ST 05	ST 06	ST 07	ST 14	ST 15	ST 16	ST 17	ST 18	ST 19	ST 20	ST 21	ET 01	ET 02	LAWV	CIG2 Center
ST05		0.49	0.18	0.04	0.03	0.01	0.01	0.01	0.01	0.01	0.02	0.09	0.17	0.02	0.31
ST06	0.27		0.57	0.06	0.03	0.01	0.01	0.01	0.01		0.01	0.12	0.26	0.02	0.11
ST07	0.13	0.58		0.11	0.06	0.02	0.02	0.01	0.01	0.01	0.01	0.21	0.38	0.04	0.04
ST14					0.76	0.48	0.40	0.33	0.26	0.21	0.17	0.74	0.16	0.67	
ST15				0.70		0.67	0.59	0.50	0.41	0.33	0.24	0.39	0.04	0.86	
ST16				0.23	0.53		0.82	0.76	0.65	0.54	0.34	0.06		0.83	
ST17				0.10	0.31	0.75		0.85	0.75	0.64	0.37	0.02		0.64	
ST18				0.02	0.11	0.54	0.77		0.85	0.77	0.38			0.34	
ST19				0.01	0.04	0.34	0.59	0.77		0.79	0.34			0.17	
ST20					0.03	0.27	0.52	0.72	0.81		0.32			0.12	
ST21				0.16	0.27	0.48	0.61	0.74	0.81	0.87		0.09	0.01	0.43	
ET01		0.01	0.03	0.75	0.56	0.29	0.24	0.19	0.15	0.13	0.11		0.53	0.44	
ET02		0.04	0.15	0.53	0.35	0.16	0.13	0.10	0.08	0.07	0.06	0.80		0.26	
LAWV				0.47	0.75	0.75	0.71	0.62	0.51	0.42	0.28	0.19	0.01		

5.0 Conclusions

An extensive number of GoldSim® and PORFLOW simulations were performed to develop a methodology for calibrating PAM to PF tracer simulation results. Overall percent errors, shown in Figure 5-1, between the calibrated GS Aquifer Model and the PF tracer simulations are less than 20% and average 4% for the 32.8-foot and 10-foot dispersivity cases. This level of agreement is considered acceptable for UQSA in the

next revision of the ELLWF PA. Larger discrepancies were observed for the 100-foot dispersivity results. However, a dispersivity of 100 ft lies at the upper end of the uncertainty range and is less likely than a dispersivity equal to 32.8 ft or 10 ft. Therefore, the lower level of agreement is acceptable for $\alpha_L = 100$ ft.

Plume overlap implementation in the system model will not utilize the built-in GS plume function because this correction factor requires calibration to the ratio between the PF-calculated plume contribution and the GS concentration. Therefore, the ratio itself will be utilized as the Plume Overlap Factor (POF). Compared to the West and Center Aquifer Models, the East Aquifer Model has consistently larger POFs with 22 factors exceeding 0.50 for the 32.8-foot dispersivity, steady-state simulations. As expected, the factors are larger where the streamtraces (Figure 2-1) for neighboring DUs are nearby. The Aquifer Model and optimized geometric parameters will be implemented in the future GS system model which will simulate subsurface flow and radionuclide transport from the ground surface to the 100-meter POA.

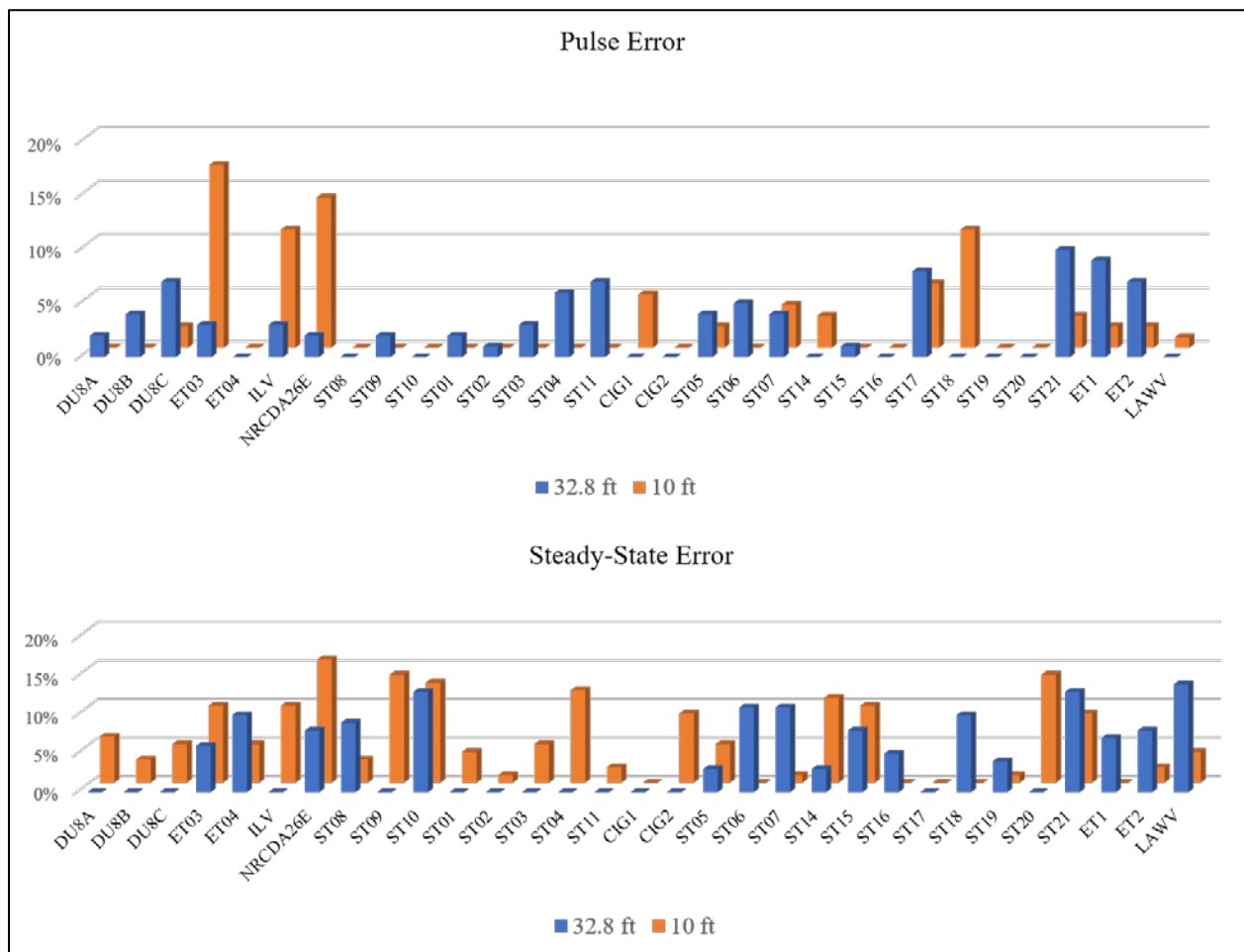


Figure 5-1. GS Aquifer Model pulse and steady-state source errors in tracer concentration compared to PF results

6.0 References

- Bagwell, L. A. and Flach, G. P. *General Separations Area (GSA) Groundwater Flow Model Update: Program and Execution Plan*. SRNL-STI-2016-00261, Revision 0. April 2016.
- Butcher, B. T. and Phifer, M. A. 2016. *Strategic Plan for Next E-Area Low-Level Waste Facility Performance Assessment*. SRNL-STI-2015-00620, Revision 0. February 2016.
- Danielson, T. *Software Quality Assurance Plan for Aquifer Model Refinement Tool (MESH3D)*. Q-SQP-G-00003, Revision 2. September 2017.
- Flach, G. P. *Recommended Aquifer Grid Resolution for E-Area PA Revision Transport Simulations*. SRNL-STI-2018-00012. January 2018a.
- Flach, G. P. *Preliminary Disposal Limits, Plume Interaction Factors, and Final Disposal Limits*. SRNL-STI-2018-00020 Rev. 0. January 2018b.
- Flach, G. P., Bagwell, L. A., and Bennett, P. L. 2017. *Groundwater Flow Simulation of the Savannah River Site General Separations Area*. SRNL-STI-2017-00008 Revision 1. September 2017.
- GTG. 2017. *GoldSim® User's Guide Version 12.0*. GoldSim® Technology Group. Issaquah, WA. February 2017.
- Hamm, L. L., Smith, F. G., Phifer, M. A., and Collard, L. B. 2009. *Savannah River Site Composite Analysis: Aquifer Flow Path Parameters*. SRNL-STI-2009-00438, Revision 0. August 2009.
- SRNL. 2009. *Savannah River Site DOE 435.1 Composite Analysis*. SRNL-STI-2009-00512, Revision 0. Savannah River Nuclear Solutions. Aiken, SC. June 2009.
- Tauxe, J. D. 2014. *Notes on the GoldSim Plume Function*. Neptune and Company, Inc. Los Alamos, NM. August 2014

Appendix A. GS Aquifer Model Pulse Source Plume Overlap Functions

Table A-1. West Aquifer Model's plume overlap factors (POF): 32.8-foot dispersivity, pulse source

	ST08	ST09	ST10	ET03	ET04	ILV	NRCDA 26E	DU8A	DU8B	DU8C	ST11 Center
ST08		0.25	0.02			0.29	0.02				
ST09	0.16		0.16			0.72					0.01
ST10		0.19				0.45					0.10
ET03	0.07	0.02			0.06	0.03	0.94			0.02	
ET04				0.52			0.04		0.01	0.37	
ILV	0.07	0.66	0.18								
NRCDA 26E	0.05	0.01		0.90	0.07	0.02				0.02	
DU8A											
DU8B					0.03			0.09			
DU8C	0.01			0.09	0.32		0.01		0.16		

Table A-2. West Aquifer Model's plume overlap factors (POF): 10-foot dispersivity, pulse source

	ST08	ST09	ST10	ET03	ET04	ILV	NRCDA 26E	DU8A	DU8B	DU8C	ST11 Center
ST08		0.08		0.01		0.15	0.02				
ST09	0.18		0.05			0.44					
ST10		0.19				0.29					0.02
ET03	0.01				0.08		0.86			0.02	
ET04				0.33			0.02		0.01	0.07	
ILV	0.09	0.42	0.07								
NRCDA 26E				0.62	0.08					0.01	
DU8A											
DU8B								0.06			
DU8C				0.03	0.11				0.11		

Table A-3. West Aquifer Model's plume overlap factors (POF): 100-foot dispersivity, pulse source

	ST08	ST09	ST10	ET03	ET04	ILV	NRCDA 26E	DU8A	DU8B	DU8C	ST11 Center	ST01 Center
ST08		0.61	0.11	0.08	0.01	0.62	0.13				0.02	
ST09	0.31		0.42			0.86	0.01				0.07	0.01
ST10	0.04	0.34				0.53					0.28	0.04
ET03	0.22	0.09	0.02		0.28	0.13	0.89			0.08		
ET04	0.04	0.02	0.00	0.61		0.03	0.26		0.06	0.68		
ILV	0.21	0.78	0.47								0.06	0.01
NRCDA 26E	0.21	0.08	0.02	0.94	0.31	0.13				0.07		
DU8A					0.01				0.01			
DU8B				0.03	0.20		0.02	0.17		0.01		
DU8C	0.03	0.01		0.27	0.64	0.02	0.11		0.23			

Table A-4. Center Aquifer Model's plume overlap factors (POF): 32.8-foot dispersivity, pulse source

	ST01	ST02	ST03	ST04	ST11	CIG1	CIG2	ST10 West	ILV West	ST05 West	ST06 West
ST01		0.22			0.16						
ST02	0.13		0.21								
ST03		0.11		0.18							
ST04			0.12			0.14					
ST11	0.28	0.01									
CIG1				0.09			0.11				
CIG2						0.12				0.11	

Table A-5. Center Aquifer Model's plume overlap factors (POF): 10-foot dispersivity, pulse source

	ST01	ST02	ST03	ST04	ST11	CIG1	CIG2	ST10 West	ILV West	ST05 West	ST06 West
ST01		0.16			0.17						
ST02	0.15		0.16								
ST03		0.14		0.15							
ST04			0.15			0.14					
ST11	0.15										
CIG1				0.13			0.11				
CIG2						0.15				0.12	

Table A-6. Center Aquifer Model's plume overlap factors (POF): 100-foot dispersivity, pulse source

	ST01	ST02	ST03	ST04	ST11	CIG1	CIG2	ST10 West	ILV West	ST05 West	ST06 West
ST01		0.42	0.05		0.31						
ST02	0.29		0.43	0.05	0.02						
ST03	0.02	0.27		0.38		0.04					
ST04		0.02	0.29			0.40	0.03				
ST11	0.53	0.09	0.01						0.03		
CIG1			0.01	0.27			0.34			0.03	
CIG2				0.02		0.39				0.32	0.02

Table A-7. East Aquifer Model's plume overlap factors (POF): 32.8-foot dispersivity, pulse source

	ST 05	ST 06	ST 07	ST 14	ST 15	ST 16	ST 17	ST 18	ST 19	ST 20	ST 21	ET 01	ET 02	LAWV	CIG2 Center
ST05		0.08													0.11
ST06	0.05		0.05										0.03		
ST07	0.00	0.13										0.01	0.08		
ST14					0.59	0.18	0.08	0.04	0.02	0.01	0.01	0.20		0.31	
ST15				0.18		0.41	0.23	0.14	0.08	0.04	0.04			0.75	
ST16					0.03		0.67	0.46	0.29	0.18	0.19			0.56	
ST17						0.75		0.71	0.47	0.31	0.35			0.07	
ST18						0.06	0.60		0.84	0.60	0.59				
ST19							0.10	0.63		0.89	0.49				
ST20							0.03	0.42	0.96		0.40				
ST21					0.01	0.10	0.16	0.24	0.31	0.38				0.04	
ET01				0.41	0.23	0.05	0.02	0.01					0.02	0.11	
ET02				0.15	0.08	0.01						0.39		0.02	
LAWV					0.53	0.65	0.38	0.25	0.15	0.09	0.08				

Table A-8. East Aquifer Model's plume overlap factors (POF): 10-foot dispersivity, pulse source

	ST 05	ST 06	ST 07	ST 14	ST15	ST 16	ST 17	ST 18	ST 19	ST 20	ST 21	ET 01	ET 02	LAWV	CIG2 Center
ST05		0.10													0.15
ST06	0.05		0.07										0.01		
ST07		0.18										0.01	0.02		
ST14					0.68	0.19	0.06	0.02	0.01			0.31		0.35	
ST15				0.17		0.51	0.24	0.10	0.04	0.01	0.01			0.86	
ST16					0.02		0.79	0.47	0.28	0.12	0.07			0.42	
ST17						0.62		0.73	0.50	0.26	0.18			0.05	
ST18						0.04	0.48		0.91	0.60	0.41				
ST19							0.08	0.49		0.90	0.36				
ST20							0.02	0.31	0.90		0.30				
ST21						0.01	0.04	0.10	0.21	0.31					
ET01				0.44	0.24	0.04	0.01						0.05	0.09	
ET02				0.11	0.06							0.32		0.02	
LAWV					0.43	0.77	0.45	0.23	0.11	0.04	0.02				

Table A-9 East Aquifer Model's plume overlap factors (POF): 100-foot dispersivity, pulse source

	ST 05	ST 06	ST 07	ST 14	ST 15	ST 16	ST 17	ST 18	ST 19	ST 20	ST 21	ET 01	ET 02	LAWV	CIG2 Center
ST05		0.28	0.02										0.02		0.32
ST06	0.24		0.27									0.01	0.05		0.01
ST07	0.01	0.41		0.01								0.04	0.13		
ST14					0.65	0.26	0.17	0.11	0.07	0.06	0.10	0.42		0.40	
ST15				0.41		0.56	0.37	0.24	0.16	0.12	0.18	0.02		0.82	
ST16					0.12		0.90	0.62	0.44	0.31	0.41			0.82	
ST17					0.01	0.99		0.87	0.64	0.46	0.56			0.29	
ST18						0.27	0.92		0.98	0.76	0.73			0.02	
ST19						0.05	0.38	0.89		0.97	0.68				
ST20						0.02	0.23	0.74	1.10		0.63				
ST21				0.02	0.08	0.32	0.41	0.45	0.48	0.50				0.20	
ET01				0.59	0.29	0.10	0.07	0.04	0.03	0.03	0.05		0.10	0.17	
ET02				0.25	0.12	0.04	0.02	0.02	0.01	0.01	0.02	0.59		0.06	
LAWV				0.06	0.68	0.82	0.57	0.38	0.26	0.18	0.26				

Intentionally Blank

Distribution:

timothy.brown@srnl.doe.gov
alex.cozzi@srnl.doe.gov
david.crowley@srnl.doe.gov
david.dooley@srnl.doe.gov
a.fellinger@srnl.doe.gov
samuel.fink@srnl.doe.gov
jeff.griffin@srnl.doe.gov
nancy.halverson@srnl.doe.gov
connie.herman@srnl.doe.gov
john.mayer@srnl.doe.gov
daniel.mccabe@srnl.doe.gov
frank.pennebaker@srnl.doe.gov
luke.reid@srnl.doe.gov
boyd.wiedenman@srnl.doe.gov
bill.wilmarth@srnl.doe.gov
erich.hansen@srnl.doe.gov
david.herman@srnl.doe.gov
Kevin.Fox@srnl.doe.gov
Gregg.Morgan@srnl.doe.gov
William.Ramsey@SRNL.DOE.gov
geoffrey.smoland@srnl.doe.gov
michael.stone@srnl.doe.gov

sebastian.aleman@srnl.doe.gov
tom.butcher@srnl.doe.gov
thomas.danielson@srnl.doe.gov
kenneth.dixon@srnl.doe.gov
james.dyer@srnl.doe.gov
gregory.flach@srnl.doe.gov
lee.fox@srs.gov
luther.hamm@srnl.doe.gov
thong.hang@srnl.doe.gov
ginger.humphries@srs.gov
roger.seitz@srnl.doe.gov
Ira.Stewart@srs.gov
kevin.tempel@srs.gov
tad.whiteside@srnl.doe.gov
jennifer.wohlwend@srnl.doe.gov
tim.coffield@srs.gov
Vijay.Jain@srs.gov
daniel.kaplan@srnl.doe.gov
Dien.Li@srs.gov
larry.romanowski@srs.gov
kent.rosenberger@srs.gov
steven.thomas@srs.gov

EM File, 773-42A – Rm. 243
(1 file copy and 1 electronic copy)
Records Administration (EDWS)